Available online at www.sciencedirect.com
SCIENCE DIRECT®
Journal of Computational Physics 205 (2005) 242–268
JOURNAL OF COMPUTATIONAL PHYSICS
www.elsevier.com/locate/jcp

An operator splitting scheme with a distributed Lagrange multiplier based fictitious domain method for wave propagation problems

Vrushali A. Bokil [a,*], Roland Glowinski [b]

[a] Center for Research in Scientific Computation, North Carolina State University, Box 8205, Raleigh, NC 27695-8205, USA
[b] Department of Mathematics, University of Houston, Houston, TX 77204-3008, USA

Received 2 March 2004; received in revised form 29 October 2004; accepted 29 October 2004
Available online 15 December 2004

Abstract

We propose a novel fictitious domain method based on a distributed Lagrange multiplier technique for the solution of the time-dependent problem of scattering by an obstacle. We study discretizations that include a fully conforming approach as well as mixed finite element formulations utilizing the lowest order Nédélec edge elements (in 2D) on rectangular grids. We also present a symmetrized operator splitting scheme for the scattering problem, which decouples the operator that propagates the wave from the operator that enforces the Dirichlet condition on the boundary of an obstacle. A new perfectly matched layer (PML) model is developed to model the unbounded problem of interest. This model is based on a formulation of the wave equation as a system of first-order equations and uses a change of variables approach that has been developed to construct PML's for Maxwell's equations. We present an analysis of our fictitious domain approach for a one-dimensional wave problem. Based on calculations of reflection coefficients, we demonstrate the advantages of our fictitious domain approach over the staircase approximation of the finite difference method. We also demonstrate some important properties of the distributed multiplier approach that are not shared by a boundary multiplier fictitious domain approach for the same problem. Numerical results for two-dimensional wave problems that validate the effectiveness of the different methods are presented.

Keywords: Fictitious domains; Perfectly matched layer; Mixed finite element methods; Operator splitting

* Corresponding author. Tel.: +1 919 513 7084; fax: +1 919 515 8967.
E-mail address: vabokil@unity.ncsu.edu (V.A. Bokil).

0021-9991/$ - see front matter © 2004 Elsevier Inc. All rights reserved.
doi:10.1016/j.jcp.2004.10.040

1. Introduction

A fictitious domain method is a technique in which the solution to a given problem is obtained by extending the given data to a larger but simpler shaped domain, containing the original domain, and solving corresponding equations in this larger *fictitious domain*. Let $\Omega \subset \mathbb{R}^d$ $(d = 1, 2, 3)$ be a domain which contains an inclusion ω as shown in Fig. 1. We consider solving for Φ in a boundary value problem of the type

$$\begin{aligned} &A(\Phi) = f, \ \text{ in } \ \Omega \setminus \bar{\omega}, \\ &B_\Gamma(\Phi) = g_0, \ \text{ on } \ \Gamma = \partial\Omega, \\ &B_{\partial\omega}(\Phi) = g_1, \ \text{ on } \ \partial\omega, \end{aligned} \tag{1}$$

where the functions f, g_0, g_1 and the operators A, B_Γ, $B_{\partial\omega}$, are known.

If Ω has a simple shape, as in Fig. 1, then we can take advantage of this by allowing the use of uniform finite difference grids or finite element meshes and hence of fast solvers for the numerical solution of the finite dimensional systems approximating (1) on such grids. To this end we replace (1) by another problem.

Find ϕ defined over Ω and M_γ a measure supported by $\partial\omega$, so that

$$\begin{aligned} &\text{(i)} \quad \widetilde{A}(\phi) = \tilde{f} + M_\gamma, \ \text{ in } \ \Omega, \\ &\text{(ii)} \quad \widetilde{B}_\Gamma(\phi) = g_0, \ \text{ on } \ \Gamma = \partial\Omega, \\ &\text{(iii)} \quad \widetilde{B}_{\partial\omega}(\phi|_{\Omega\setminus\bar{\omega}}) = g_1, \ \text{ on } \ \partial\omega, \end{aligned} \tag{2}$$

where the operator $\widetilde{A}$ is of the same type as A and coincides (in some sense) with A on $\Omega \setminus \bar{\omega}$, $\tilde{f}$ is some extension of f over Ω and $\widetilde{B}_\Gamma$, and $\widetilde{B}_{\partial\omega}$ are extensions of B_Γ, and $B_{\partial\omega}$, respectively. If we choose the measure M_γ so that the solution of (2, i, ii) satisfies relation (2, iii) then we can expect to have $\phi|_{\Omega\setminus\bar{\omega}} = \Phi$.

Fictitious domain methods can be traced back to the 1960s to Saul'ev [1]. The fictitious domain can be a rectangle or a circle, for example. The advantage of this method is that the problem in the fictitious domain can be discretized on a uniform mesh, independent of the boundary of the original domain, thus avoiding the time consuming construction of a boundary fitted mesh as in the finite element method. (However, there are some classes of fictitious domain methods that use boundary fitted meshes to improve accuracy [2].) At the same time, such an approach is more accurate than the staircase approximation of the finite difference method.

A fictitious domain method is also known as a *domain imbedding method* [3] or a *fictitious component method* [4]. A related technique is the *capacitance matrix method* [5,6]. One class of fictitious domain

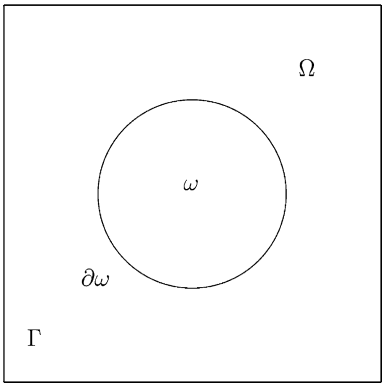

Fig. 1. The obstacle ω embedded inside the larger domain Ω.

methods involves using *distributed/boundary Lagrange multipliers* to enforce the boundary conditions on the boundaries of the original smaller domain. This is known as the *functional analytic approach*; it leads to *saddle point problems* and has been considered jointly by Glowinski et al. [7,8] and by Kuznetsov [9–11] among others. This is the class of methods that we will consider in this paper. The functional analytic approach was originally developed to handle problems with complex geometries in the stationary case [8,12]. The application of this approach to time dependent problems is relatively new and has recently been studied by Glowinski and Joly among others [13–16].

There are other classes of fictitious domain methods. We will mention some of these briefly. One class of methods uses an *optimal control* approach [17,18]. In this approach, the system is solved in the fictitious domain, with a distributed/boundary control introduced on the right hand side of the system equations. The control forces the solution to satisfy the required boundary conditions, at least approximately. This approach resembles the Lagrange multiplier technique. In some cases the solution of the optimal control problem is obtained by solving the optimality conditions. The cost function here consists of two parts; one part penalizes the boundary condition and the other part penalizes the control inside the original domain/boundary [18]. This leads to an optimization problem. Fictitious domain methods are often used to construct a preconditioner for iterative methods such as *Krylov subspace methods*. One such approach is called an *algebraic* fictitious domain method [4,2].

In this paper, we will apply a distributed Lagrange multiplier based fictitious domain method to a time-dependent scattering problem. For problem (2), this approach implies finding a measure M_ω supported over the domain ω instead of just the boundary γ, and satisfying the Eq. (2, iii) on ω instead of γ. We consider the scalar wave equation with constant coefficients. We are interested in studying the scattering of a wave by an obstacle $\omega \subset \mathbb{R}^d$ with $d = 2$ (or $d = 3$). Let c denote the speed of propagation. The scalar evolution problem is to find Φ such that:

$$
\begin{aligned}
&\text{(i)} && \frac{1}{c^2}\frac{\partial^2 \Phi}{\partial t^2} - \Delta \Phi = 0, \ \text{ in } \ \Omega \setminus \bar{\omega},\\
&\text{(ii)} && \Phi = G, \ \text{ on } \ \partial\omega,\\
&\text{(iii)} && \frac{1}{c}\frac{\partial \Phi}{\partial t} + \frac{\partial \Phi}{\partial \mathbf{n}} = 0, \quad \text{on } \ \Gamma = \partial\Omega,\\
&\text{(iv)} && \Phi(0) = \Phi_0, \ \frac{\partial \Phi}{\partial t}(0) = \Phi_1.
\end{aligned}
\tag{3}
$$

In Fig. 1, ω is a disk which is embedded in the larger bounded rectangular domain Ω of $\mathbb{R}^2$, and $\mathbf{n}$ is the unit outward normal vector to the boundary $\partial\Omega$.

In Section 2, we describe our fictitious domain method and present energy decay results. In Sections 3 and 4, we describe a fully conforming approach and a mixed finite element approach, respectively, for the numerical solution of the scattering problem (3). In both cases, we will use finite elements for spatial discretization and finite differences for the temporal discretizations. The main advantage of the fictitious domain method is that the discretization of the fictitious domain is independent of the geometry of the obstacle, hence we can use uniform meshes in our discretizations. Section 5 discusses the iterative solution of the resulting equations. In Section 6, we perform stability analyses on the methods described in Sections 3 and 4 via the definition of discrete energies and energy decay results. These analyses demonstrate another important aspect of our fictitious domain method, namely the independence of the stability condition (CFL) on the presence (or absence) of obstacles. In Section 7, we describe an operator splitting scheme for the numerical solution of problem (3), which decouples the operator that propagates the wave from the operator that enforces the Dirichlet condition on the boundary of the obstacle. The main idea behind such a splitting is that each *subproblem* in the full scheme corresponds to only one operator and hence is quite trivial to solve. This allows us to use different discretizations for the different subproblems [19,20].

We also show, via numerical examples, that the operator splitting scheme performs as well as the scheme without splitting.

We would like to study problem (3, i, iv) with the constraint (3, ii) in the case of an unbounded exterior domain, i.e., in $\mathbb{R}^2 \setminus \bar{\omega}$, instead of a finite domain $\Omega \setminus \bar{\omega}$. One of the ways of simulating the scattering problem in an unbounded domain is to impose an absorbing boundary condition on the boundary of the truncated domain Ω. Hence, we consider a finite domain Ω, and we impose a first-order absorbing boundary condition (3, iii) on the (artificial) boundary Γ. In Section 8, we will construct a more accurate technique called a *perfectly matched layer* method to simulate such unbounded wave propagation problems. In Section 9, we perform numerical results to validate the different models presented.

One of the methods used to solve time dependent problems of scattering by an obstacle, such as (3), is the finite difference method, which uses a rectangular grid, an explicit scheme in time and approximates the obstacle in a staircase fashion as shown in Fig. 2. In this figure the scattering obstacle is a disk, and is approximated by another object as shown. The finite difference method is computationally easy to implement, but its staircase approximation is not accurate. In Section 10 we will show, via a 1D analysis, that our distributed Lagrange multiplier based fictitious domain method is a much more accurate and efficient method for solving time dependent problems like (3). We will also demonstrate that the distributed multiplier approach has certain desirable properties which are lacking in a boundary multiplier approach [13,15] for the same problem.

2. A fictitious domain formulation for the wave problem

In this section, we describe a distributed Lagrange multiplier based fictitious domain method to solve the time dependent scattering problem (3). The idea behind our fictitious domain method is to extend the solution Φ of problem (3) inside the obstacle ω, and solve the wave equation in the entire domain Ω, which has a simple shape like a square or rectangle [13–16]. The Dirichlet condition on $\partial\omega$, (3, ii), is enforced via the introduction of a distributed Lagrange multiplier on the domain ω. In [13,15] a boundary multiplier fictitious domain method is introduced for the wave equation and for Maxwell's equations. Distributed multiplier based fictitious domain methods have been used for the numerical solution of elliptic problems [10], for the Stokes problem [21] and for particulate flows in [7,22]. Thus, this paper extends the applicability of this approach to wave propagation problems.

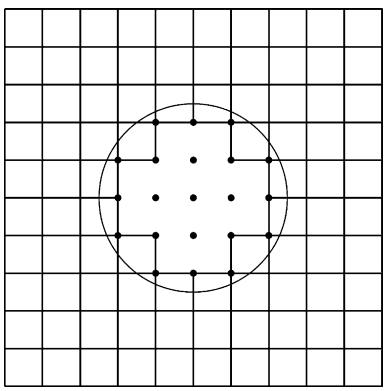

Fig. 2. A staircase approximation (highlighted nodal points) to a scattering disk.

Let g be an H^1-extension of G on ω in (3, ii). Using a distributed Lagrange multiplier approach problem (3) is equivalent, at least formally, to the following variational one:

Find $\{\phi(t),\lambda(t)\} \in H^1(\Omega)\times L^2(\omega)$ such that

$$\begin{aligned}
&\text{(i)} \quad \frac{1}{c^2}\int_\Omega \frac{\partial^2\phi}{\partial t^2} w\,\mathrm{d}x + \int_\Omega \nabla\phi\cdot\nabla w\,\mathrm{d}x + \frac{1}{c}\int_\Gamma \frac{\partial\phi}{\partial t} w\,\mathrm{d}\Gamma + \int_\omega \lambda w\,\mathrm{d}\omega = 0 \quad \forall w \in H^1(\Omega),\\
&\text{(ii)} \quad \int_\omega (\phi - g)\mu\,\mathrm{d}\omega = 0 \quad \forall \mu \in L^2(\omega),\\
&\text{(iii)} \quad \phi(0) = \phi_0,\ \frac{\partial\phi}{\partial t}(0) = \phi_1,
\end{aligned} \tag{4}$$

in the sense that

$$\phi = \begin{cases} \Phi \text{ on } \Omega\setminus\bar{\omega}, \\ G \text{ on } \partial\omega. \end{cases} \tag{5}$$

The function ϕ_0 is chosen to be an H^1-extension of Φ_0, and ϕ_1 to be at least an L^2-extension of Φ_1.

Equivalently, we can construct another fictitious domain method for the wave problem (3) by writing it in first-order form. To this end let us define the time derivative u and the gradient $\mathbf{p}$ as

$$u = \frac{\partial\phi}{\partial t}, \quad \mathbf{p} = \nabla\phi. \tag{6}$$

Rewriting the wave equation as a system of first-order PDE's by the use of the variables u and $\mathbf{p}$, we construct the following fictitious domain formulation of the wave problem as

Find $\{\phi(t), u(t), \mathbf{p}(t), \lambda(t)\} \in H^1(\Omega)\times H^1(\Omega)\times [L^2(\Omega)]^2 \times L^2(\omega)$ such that:

$$\begin{aligned}
&\text{(i)} \quad \frac{\partial\phi}{\partial t} - u = 0,\\
&\text{(ii)} \quad \frac{1}{c^2}\int_\Omega \frac{\partial u}{\partial t} w\,\mathrm{d}x + \int_\Omega \mathbf{p}\cdot\nabla w\,\mathrm{d}x + \frac{1}{c}\int_\Gamma u w\,\mathrm{d}\Gamma + \int_\omega \lambda w\,\mathrm{d}\omega = 0 \quad \forall w \in H^1(\Omega),\\
&\text{(iii)} \quad \int_\Omega \frac{\partial\mathbf{p}}{\partial t}\cdot\mathbf{q}\,\mathrm{d}x - \int_\Omega \nabla u\cdot\mathbf{q}\,\mathrm{d}x = 0 \quad \forall \mathbf{q} \in [L^2(\Omega)]^2,\\
&\text{(iv)} \quad \int_\omega (u - \frac{\partial g}{\partial t})\mu\,\mathrm{d}\omega = 0 \quad \forall \mu \in L^2(\omega),\\
&\text{(v)} \quad \phi(0) = \phi_0,\ u(0) = \phi_1,\ \mathbf{p}(0) = \nabla\phi_0,
\end{aligned} \tag{7}$$

in a similar sense to (5). We note that the Dirichlet boundary condition is imposed on u and not on ϕ as in (4). Also, (7, i) is posed in a strong sense as ϕ and u are in the same space. One of the advantages of considering a mixed formulation of the wave equation is the ease of constructing a perfectly matched layer (PML) model for the absorption of outgoing waves. PML model's have been shown to provide excellent absorbing capabilities for wave problems. Another advantage of such a formulation is that we can obtain information about the gradient directly. In the numerical approximation of formulation (7) we will employ a discretization in which the degrees of freedom for u and $\mathbf{p}$ are staggered in space and time as in the FDTD scheme that is very popular for Maxwell's equations [23,24].

2.1. Energy decay

In this section, we derive *energy identities* from the variational formulations (4) and (7). The energy identities presented below guarantee the well-posedness of the problems and the stability of the solutions.

Theorem 1. *Let us assume that* $g = 0$ *in* (4, ii). *Then, system* (4) *verifies the energy identity*

$$\frac{\mathrm{d}}{\mathrm{d}t}\mathscr{E}_{\mathrm{C}} = -\frac{1}{c}\left\|\frac{\partial\phi}{\partial t}\right\|^2_{L^2(\Gamma)}, \tag{8}$$

where the energy $\mathscr{E}_{\mathrm{C}}$ *is defined as*

$$\mathscr{E}_{\mathrm{C}} = \frac{1}{2}\left\{\frac{1}{c^2}\left\|\frac{\partial\phi}{\partial t}\right\|^2_{L^2(\Omega)} + \|\nabla\phi\|^2_{L^2(\Omega)}\right\}, \tag{9}$$

with $\|\cdot\|^2_{L^2(\Gamma)} = \int_\Gamma|\cdot|^2\,\mathrm{d}\Gamma$, *and* $\|\cdot\|^2_{L^2(\Omega)} = \int_\Omega|\cdot|^2\,\mathrm{d}x$. *Thus,* (8) *implies that the energy does not grow over time, i.e.*

$$\mathscr{E}_{\mathrm{C}}(t) \leqslant \mathscr{E}_{\mathrm{C}}(0) \quad \forall t > 0. \tag{10}$$

Eq. (8) *implies that there is no dissipation of the waves in the domain* Ω. *This is the principle of conservation of energy for the wave equation.*

Proof. Let us take $w = \frac{\partial\phi}{\partial t}$ in (4, i). We obtain

$$\frac{1}{2}\frac{\mathrm{d}}{\mathrm{d}t}\left\{\frac{1}{c^2}\left\|\frac{\partial\phi}{\partial t}\right\|^2_{L^2(\Omega)} + \|\nabla\phi\|^2_{L^2(\Omega)}\right\} + \frac{1}{c}\int_\Gamma\left|\frac{\partial\phi}{\partial t}\right|^2\mathrm{d}\Gamma + \int_\omega\lambda\frac{\partial\phi}{\partial t}\,\mathrm{d}\omega = 0. \tag{11}$$

From (4, ii) with $g = 0$, by differentiating with respect to time and then choosing $\mu = \lambda$, we have

$$\int_\omega\frac{\partial\phi}{\partial t}\lambda\,\mathrm{d}\omega = 0. \tag{12}$$

Substituting (12) in (11), and using the definition (9) gives us (8). □

Theorem 2. *Let us assume that* $g = 0$ *in* (7, iv). *Then, system* (7) *verifies the energy identity*

$$\frac{\mathrm{d}}{\mathrm{d}t}\mathscr{E}_M = -\frac{1}{c}\|u\|^2_{L^2(\Gamma)}, \tag{13}$$

where the energy $\mathscr{E}_M$ *is defined as*

$$\mathscr{E}_M = \frac{1}{2}\left\{\frac{1}{c^2}\|u\|^2_{L^2(\Omega)} + \|\mathbf{p}\|^2_{L^2(\Omega)}\right\}. \tag{14}$$

As before, (13) *implies that the energy does not grow over time, i.e.*

$$\mathscr{E}_M(t) \leqslant \mathscr{E}_M(0) \quad \forall t > 0. \tag{15}$$

Proof. Let us take $w = u$ in (7, ii), and $\mathbf{q} = \mathbf{p}$ in (7, iii), and add the two resulting equations. This gives us

$$\frac{1}{2}\frac{\mathrm{d}}{\mathrm{d}t}\left\{\frac{1}{c^2}\|u\|^2_{L^2(\Omega)} + \|\mathbf{p}\|^2_{L^2(\Omega)}\right\} + \frac{1}{c}\int_\Gamma|u|^2\mathrm{d}\Gamma + \int_\omega\lambda u\,\mathrm{d}\omega = 0. \tag{16}$$

From (7, iv), with $g = 0$, choosing $\mu = \lambda$ we have

$$\int_\omega u\lambda\,\mathrm{d}\omega = 0. \tag{17}$$

Substituting (17) in (16), and using the definition (14) gives us (13). □

3. A fully conforming method for the numerical solution of the wave problem

We will use finite elements in space and finite differences in time for the numerical approximations of both (4) and (7). As mentioned in Section 1, the advantage of the fictitious domain formulation is that we can use uniform meshes to discretize the problems. In the following subsections we present details regarding the numerical approximation of problem (4).

3.1. Time discretization

We will use a centered finite difference scheme for the time discretization of the wave problem. On the interval $[0,T]$, let $\Delta t = T/N$ be the time step, where $N \in \mathbb{N}$. Define $\phi^k \approx \phi(k\Delta t)$ and denote $t^k = k\Delta t$, for $k \in \mathbb{Z}$.

For $n = 0, 1, \ldots, N-1$, on the interval (t^n, t^{n+1}), given ϕ^n, ϕ^{n-1} we will solve the problem:

Find $(\phi^{n+1}, \lambda^{n+1}) \in H^1(\Omega) \times L^2(\omega)$ such that

$$\begin{aligned}
&\text{(i)} \quad \frac{1}{c^2}\int_\Omega \frac{\phi^{n+1} - 2\phi^n + \phi^{n-1}}{\Delta t^2} w \,\mathrm{d}x + \int_\Omega \nabla\phi^n \cdot \nabla w \,\mathrm{d}x + \int_\omega \lambda^{n+1} w \,\mathrm{d}\omega \\
&\qquad + \frac{1}{c}\int_\Gamma \frac{\phi^{n+1} - \phi^{n-1}}{2\Delta t} w \,\mathrm{d}\Gamma = 0 \quad \forall w \in H^1(\Omega), \\
&\text{(ii)} \quad \int_\omega (\phi^{n+1} - g^{n+1})\mu \,\mathrm{d}\omega = 0 \quad \forall \mu \in L^2(\omega), \\
&\text{(iii)} \quad \phi^0 = \phi_0, \;\; \phi^1 = \phi^{-1} + 2\Delta t \phi_1.
\end{aligned} \tag{18}$$

3.2. Finite element approximation of the wave problem

This is one of the most important sections in this paper as it describes how the Dirichlet boundary condition is numerically enforced. We divide Ω into elementary rectangles, and consider $\mathscr{T}_h$ to be a uniform mesh with elements $\{K\}$ of edge length h. We define the finite dimensional space

$$\mathbf{V}_h = \left\{ v_h | v_h \in C^0(\overline{\Omega}), v_h|_K \in Q_1 \quad \forall K \in \mathscr{T}_h \right\}, \tag{19}$$

which approximates $H^1(\Omega)$. In (19), the space Q_1 is defined as $Q_1 = P_{11}$, where, for $k_1,\ k_2 \in \mathbb{N} \cup \{0\}$

$$P_{k_1 k_2} = \left\{ p(x_1, x_2) | p(x_1, x_2) = \sum_{0 \leqslant i \leqslant k_1} \sum_{0 \leqslant j \leqslant k_2} a_{ij} x_1^i x_2^j,\ a_{ij} \in \mathbb{R} \right\}. \tag{20}$$

Thus, P_{11} is the space of the bilinear functions of two variables, and $\mathbf{V}_h$ is the space of continuous piecewise bilinear functions. Since $\phi \in H^1(\Omega)$ (which is its natural space), we will choose the space $\mathbf{V}_h$ for the finite element approximation ϕ_h of ϕ.

We will also use mass-lumping for the calculation of the integrals

$$\int_\Omega v_h w_h \,\mathrm{d}x = \sum_{K \in \mathscr{T}_h} \int_K v_h w_h \,\mathrm{d}x \quad \forall v_h, w_h \in \mathbf{V}_h, \tag{21}$$

due to which we obtain a diagonal mass matrix leading to an explicit scheme in time. Similarly, we use mass-lumping to calculate the boundary integral $\int_\Gamma v_h w_h \,\mathrm{d}\Gamma$.

Let the set of mesh points on $\overline{\Omega}$ be defined as

$$\Sigma_h = \left\{ P | P \in \overline{\Omega},\ P \text{ is a vertex of } \mathscr{T}_h \right\}. \tag{22}$$

Next, we define the set

$$\Sigma_h^{\bar{\omega}} = \{P | P \in \bar{\omega},\ d(P, \partial\omega) \geqslant h\} \cup \text{Discrete set of points belonging to } \partial\omega, \tag{23}$$

where $d(P, \partial\omega)$ is the distance of the point P from the boundary $\partial\omega$. The points on $\partial\omega$ are typically chosen so that their distance is of the order of h. See Fig. 3. Using the sets defined above, we now define the set $\mathbf{\Lambda}_h$ of the Lagrange multipliers by

$$\mathbf{\Lambda}_h = \left\{ \mu_h | \mu_h = \sum_{P \in \Sigma_h^{\bar{\omega}}} \mu_P \chi_P,\ \mu_P \in \mathbb{R} \right\}, \tag{24}$$

with χ_P the characteristic function of the elementary square of center P and edge length h; we clearly have $\mu_h(P) = \mu_P$. We approximate the integrals involving the distributed multiplier by

$$\int_\omega \mu_h v_h \, \mathrm{d}x \approx h^2 \sum_{P \in \Sigma_h^{\bar{\omega}}} \mu_h(P) v_h(P) \quad \forall v_h \in \mathbf{V}_h,\ \forall \mu_h \in \mathbf{\Lambda}_h. \tag{25}$$

Fig. 3 illustrates the degrees of freedom for the solution ϕ (left), and a choice for the set $\Sigma_h^{\bar{\omega}}$ in the case of a scattering disk. In this figure, the ratio of the distance between points on the circle, denoted by $h_{\partial\omega}$, to the mesh step size h is about 1.3. We will call this ratio as the *mesh ratio*. In numerical experiments, good results are observed when the mesh ratio is approximately 1.5 [25].

Using the above definitions, a fully discretized scheme for the wave problem is given by the following fully discrete variational formulation.

• **Scheme** FDDM:

Find $(\phi_h^{n+1}, \lambda_h^{n+1}) \in \mathbf{V}_h \times \Lambda_h$ such that:

$$\begin{aligned}
&\text{(i)} \quad \frac{1}{c^2} \int_\Omega \frac{\phi_h^{n+1} - 2\phi_h^n + \phi_h^{n-1}}{\Delta t^2} w_h \, \mathrm{d}x + \int_\Omega \nabla \phi_h^n \cdot \nabla w_h \, \mathrm{d}x + \frac{1}{c} \int_\Gamma \frac{\phi_h^{n+1} - \phi_h^{n-1}}{2\Delta t} w_h \, \mathrm{d}\Gamma \\
&\qquad + \int_\omega \lambda_h^{n+1} w_h \, \mathrm{d}\omega = 0 \quad \forall w_h \in \mathbf{V}_h, \\
&\text{(ii)} \quad \int_\omega (\phi_h^{n+1} - g^{n+1}) \mu_h \, \mathrm{d}\omega = 0 \quad \forall \mu_h \in \mathbf{\Lambda}_h, \\
&\text{(iii)} \quad \phi_h^0 = \phi_0,\ \phi_h^1 = \phi_h^{-1} + 2\Delta t \phi_1.
\end{aligned} \tag{26}$$

We will discuss the iterative solution of (26) in Section 5.

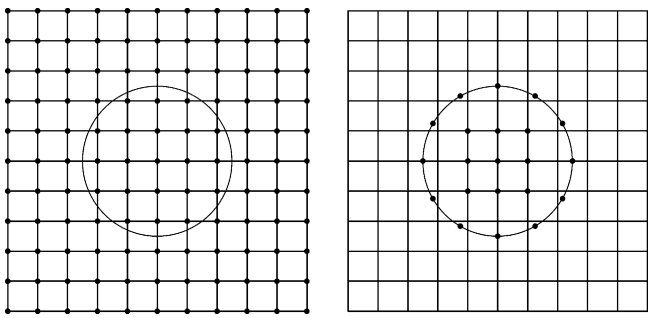

Fig. 3. The degrees of freedom for the solution ϕ (left), and the degrees of freedom, $\Sigma_h^{\bar{\omega}}$, for the Lagrange multiplier λ (right) in the fictitious domain method for the case of a scattering disk. The mesh ratio, i.e., the ratio of the step size chosen on the boundary of the disk to the mesh step size, is about 1.3.

4. A mixed finite element method for the numerical solution of the wave problem

In this section, we present a mixed finite element method for approximating the variational formulation (7). The approximation of ϕ,u and λ are carried out as detailed in the previous section. Since $\phi_h \in Q_1$ on any $K \in \mathscr{T}_h$, we will choose a finite element space $\mathbf{P}_h$ for the approximation of $\mathbf{p}$ such that the reference space for this approximation is

$$P_{01} \times P_{10} \supset \nabla Q_1, \tag{27}$$

in order that we can construct the space $\mathbf{P}_h$ such that

$$\nabla \mathbf{V}_h \subset \mathbf{P}_h. \tag{28}$$

By satisfying (28), we ensure the validity of an *inf–sup* condition related to the inner product $\int_\Omega \mathbf{q}_h \cdot \nabla w_h \, dx \quad \forall \mathbf{q}_h \in \mathbf{P}_h, \ \forall w_h \in \mathbf{V}_h$ (see sufficient conditions for convergence of mixed methods discussed in [26]). Thus, the approximation space $\mathbf{P}_h$, for the approximation of $\mathbf{p}$, is chosen to be

$$\mathbf{P}_h = \left\{ \mathbf{q} \in [L^2(\Omega)]^2 | \forall K \in \mathscr{T}_h, \ \mathbf{q}|_K \in P_{01} \times P_{10} \right\}. \tag{29}$$

This space of linear edge elements for the gradient can be seen as the lowest order Nédélec space in two-dimensions (Nédélec's results are for 3D). The degrees of freedom for the approximations ϕ_h, u_h and of $\mathbf{p}_h = (p_{x,h}, p_{y,h})^{\mathrm{T}}$ are staggered in both time and space as shown in Fig. 4. The degrees of freedom for $p_{x,h}$ and $p_{y,h}$ are at the midpoints of edges parallel to the x-axis and y-axis, respectively.

As before, we will use a centered finite difference scheme for the time discretization of the wave problem. On the interval $[0, T]$, let $\Delta t = T/N$ be the time step, where $N \in \mathbb{N}$. Define $t^j = j\Delta t$, and $\phi^j \approx \phi(t^j)$, where $j = k$ or $j = k + 1/2$, for $k \in \mathbb{N}$.

• **Scheme** MDM:

Find $(\phi_h^{n+1}, u_h^{n+1}, \mathbf{p}_h^{n+1/2}, \lambda_h^{n+1}) \in \mathbf{V}_h \times \mathbf{V}_h \times \mathbf{P}_h \times \mathbf{\Lambda}_h$ such that:

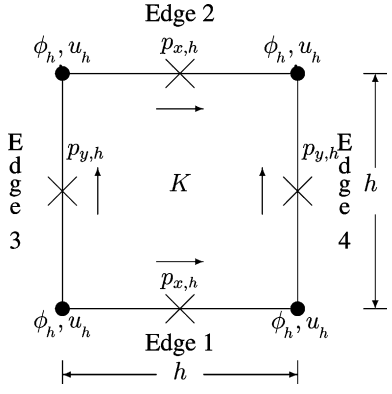

Fig. 4. A sample domain element K.

$$
\begin{aligned}
&\text{(i)} && \frac{\phi_h^{n+1}-\phi_h^n}{\Delta t} = u_h^n,\\
&\text{(ii)} && \int_\Omega \frac{\mathbf{p}_h^{n+1/2}-\mathbf{p}_h^{n-1/2}}{\Delta t}\mathbf{q}_h\,\mathrm{d}x - \int_\Omega \mathbf{q}_h\cdot\nabla u_h^n\,\mathrm{d}x = 0 \quad \forall \mathbf{q}_h \in \mathbf{P}_h,\\
&\text{(iii)} && \frac{1}{c^2}\int_\Omega \frac{u_h^{n+1}-u_h^n}{\Delta t} w_h\,\mathrm{d}x + \int_\Omega \mathbf{p}_h^{n+1/2}\cdot\nabla w_h\,\mathrm{d}x + \frac{1}{c}\int_\Gamma \frac{u_h^{n+1}+u_h^n}{2} w_h\,\mathrm{d}\Gamma\\
&&& \quad + \int_\omega \lambda_h^{n+1} w_h\,\mathrm{d}\omega = 0 \quad \forall w_h \in \mathbf{V}_h,\\
&\text{(iv)} && \int_\omega (u_h^{n+1}-g^{n+1})\mu_h\,\mathrm{d}\omega = 0 \quad \forall \mu_h \in \mathbf{\Lambda}_h,\\
&\text{(v)} && \phi_h^0 = \phi_0,\ u_h^0 = \phi_1,\ \mathbf{p}_h^{-1/2} = \nabla\phi_0 - \frac{\Delta t}{2}\nabla\phi_1.
\end{aligned}
\tag{30}
$$

As done in Section 3.2, we will mass-lump the integrals involved above. Since we are using uniform meshes this should not pose any difficulties. In the numerical solution of (30) we will solve for ϕ_h^{n+1} from (30, i), then we will solve for $\mathbf{p}_h^{n+1/2}$ from (30, ii). Both these steps are explicit in time. We will then solve (30, iii) and (30, iv) iteratively as described in Section 5.

5. Iterative solution of the discrete problem

For the solution of the system (26, i, ii) or (30, iii, iv) at each time step, we have to solve a system of linear equations of the saddle point form

$$
\begin{aligned}
&D_h\psi_h^{n+1} + B_h^{\mathrm{T}}\lambda_h^{n+1} = a,\\
&B_h\psi_h^{n+1} = b,
\end{aligned}
\tag{31}
$$

where $\psi_h^{n+1} = \phi_h^{n+1}$ in (26) and $\psi_h^{n+1} = u_h^{n+1}$ in (30). Also $D_h \in \mathbb{R}^{N\times N}$ is a diagonal mass matrix, and $B_h \in \mathbb{R}^{M\times N}(M \ll N)$. We use the *Schur Complement* of the system (31) that is, we solve

$$
\left(B_h D_h^{-1} B_h^{\mathrm{T}}\right)\lambda_h^{n+1} = B_h D_h^{-1} a - b,
\tag{32}
$$

for λ_h^{n+1}. We do this by using a conjugate gradient algorithm in the form given by Glowinski and LeTallec [27].

We note that the matrix $B_h D_h^{-1} B_h^{\mathrm{T}}$ is symmetric and positive definite. This property is related to a uniform discrete inf–sup condition associated with the integral $\int_\omega v\mu\mathrm{d}\omega \quad \forall v \in \mathbf{V}_h,\ \forall \mu \in \mathbf{\Lambda}_h$.

As mentioned in Section 1, we again note that the mesh grid in the fictitious domain and the degrees of freedom on the boundary of the obstacle are chosen independently of each other, except that the boundary mesh size is larger than the mesh size in the domain. In [25], the authors derive error estimates for a fictitious domain method for elliptic problems with non-homogeneous boundary conditions, provided that the ratio between the boundary mesh size and the mesh size in the domain, i.e., what we call the mesh ratio $h_{\partial\omega}/h$, is approximately two or three. The crucial step is the proof of a uniform discrete inf–sup condition via the construction of a suitable restriction operator. However, this restriction on the mesh ratio is only sufficient and good numerical results are obtained when this ratio is approximately 1.5 as is demonstrated by the numerical results presented in [16,8] and as will be seen in this paper.

6. Decay of discrete energies and stability analysis

Analogously to the continuous case, we derive *discrete* energy identities based on the discrete variational formulations (26) and (30). Using these identities we show that the respective fictitious domain formulations are stable, with the Courant–Friedrichs–Lewy (CFL) stability condition being the same as in the case of the problem without an obstacle. We will assume that $g = 0$ in (26, ii) and in (30, iv). We define the bilinear form

$$a(\phi_h, \psi_h) = \int_\Omega \nabla\phi_h \cdot \nabla\psi_h \, \mathrm{d}x \quad \forall (\phi_h, \psi_h) \in \mathbf{V}_h \times \mathbf{V}_h, \tag{33}$$

and the operator $\mathscr{A}_h : \mathbf{V}_h \to \mathbf{V}_h'$ by

$$(\mathscr{A}_h \phi_h, \psi_h)_{L^2(\Omega)} = a(\phi_h, \psi_h). \tag{34}$$

Let I be the identity operator on $\mathbf{V}_h$.

Theorem 3. *If the CFL condition $c\Delta t \leqslant h/\sqrt{2}$ is satisfied (in 2D), then the operator*

$$\mathscr{S}_h = I - \frac{c^2\Delta t^2}{4}\mathscr{A}_h, \tag{35}$$

defines a positive quadratic form, the expression

$$\mathscr{E}_h^{n+1/2} = \frac{1}{2}\left\{\frac{1}{c^2}\left(\frac{\phi_h^{n+1} - \phi_h^n}{\Delta t}, \mathscr{S}_h\frac{\phi_h^{n+1} - \phi_h^n}{\Delta t}\right) + \left\|\nabla\left(\frac{\phi_h^{n+1} + \phi_h^n}{2}\right)\right\|^2\right\}, \tag{36}$$

defines a discrete energy, and system (26) verifies the energy identity

$$\mathscr{E}_h^{n+1/2} = \mathscr{E}_h^{n-1/2} - \frac{\Delta t}{c}\left\|\frac{\phi_h^{n+1} - \phi_h^{n-1}}{2\Delta t}\right\|^2_{L^2(\Gamma)} \quad \forall n \in \mathbb{N},\ \ n \geqslant 0. \tag{37}$$

Thus, (37) implies that the discrete energy does not grow over time, i.e.

$$\mathscr{E}_h^{n+1/2} \leqslant \mathscr{E}_h^{n-1/2} \quad \forall n \geqslant 0. \tag{38}$$

Proof. Using the definition of the operator $\mathscr{A}_h$ we can rewrite the discrete energy as

$$\mathscr{E}_h^{n+1/2} = \frac{1}{2}\left\{\frac{1}{c^2}\left\|\frac{\phi_h^{n+1} - \phi_h^n}{\Delta t}\right\|^2 + \int_\Omega \nabla\phi_h^{n+1} \cdot \nabla\phi_h^n \, \mathrm{d}x\right\}. \tag{39}$$

From (26, i) taking $w_h = \frac{\phi_h^{n+1} - \phi_h^{n-1}}{2\Delta t}$, and using the definition (36) we obtain

$$\frac{\mathscr{E}_h^{n+1/2} - \mathscr{E}_h^{n-1/2}}{\Delta t} + \frac{1}{2\Delta t}\int_\omega \lambda_h^{n+1}\left(\phi_h^{n+1} - \phi_h^{n-1}\right)\mathrm{d}\omega = -\frac{1}{c}\left\|\frac{\phi_h^{n+1} - \phi_h^{n-1}}{2\Delta t}\right\|^2_{L^2(\Gamma)}. \tag{40}$$

Next, from (26, ii) by taking $\mu_h = \lambda_h^{n+1}$, and $\mu_h = \lambda_h^{n+3}$ we have, respectively

$$\int_\omega \lambda_h^{n+1}\phi_h^{n+1}\,\mathrm{d}x = 0 \quad \text{and} \quad \int_\omega \lambda_h^{n+1}\phi_h^{n-1}\,\mathrm{d}x = 0. \tag{41}$$

Substituting (41) in (40) we obtain the energy identity (37).

It remains to show that the operator $\mathscr{S}_h$ defines a positive quadratic form under the given CFL condition. In two dimensions we have [28]

$$\sup_{w_h \in \mathbf{V}_h} \frac{h^2 (\mathscr{A}_h w_h, w_h)_{L^2(\Omega)}}{4 (w_h, w_h)_{L^2(\Omega)}} < 2, \tag{42}$$

which along with the CFL condition implies that

$$(w_h, \mathscr{S}_h w_h)_{L^2(\Omega)} = (w_h, (I - \frac{c^2 \Delta t^2}{4} \mathscr{A}_h) w_h)_{L^2(\Omega)} > 0 \quad \forall w_h \in \mathbf{V}_h \setminus \{0\}. \tag{43}$$

Eq. (43) implies that the operator $\mathscr{S}_h$ is positive definite. Thus, the CFL condition assures the stability of the scheme (26). We note that the CFL condition is not affected by the presence of the obstacle, i.e., the stability condition for the distributed multiplier based fictitious domain method is the same as that for the finite difference method. This is also true in the case of a boundary multiplier based fictitious domain method, as is noted in [14]. □

Theorem 4. *If the CFL condition, $c\Delta t \leqslant h/\sqrt{2}$ is satisfied, then the operator $\mathscr{S}_h$ defined in (35) defines a positive quadratic form, the expression*

$$\mathscr{E}_h^{n+1/2} = \frac{1}{2} \left\{ \frac{1}{c^2} \left(u_h^{n+1}, \mathscr{S}_h u_h^{n+1} \right)_{L^2(\Omega)} + \left\| \left(\frac{\mathbf{p}_h^{n+1/2} + \mathbf{p}_h^{n-1/2}}{2} \right) \right\|_{L^2(\Omega)}^2 \right\} \tag{44}$$

defines a discrete energy, and system (30) verifies the energy identity

$$\mathscr{E}_h^{n+1/2} = \mathscr{E}_h^{n-1/2} - \frac{\Delta t}{c} \left\| \frac{u_h^{n+1} + u_h^n}{2} \right\|_{L^2(\Gamma)}^2 \quad \forall n \in \mathbb{N}, \ \ n \geqslant 0. \tag{45}$$

Thus, (45) implies that the discrete energy does not grow over time, i.e.

$$\mathscr{E}_h^{n+1/2} \leqslant \mathscr{E}_h^{n-1/2} \quad \forall n \geqslant 0. \tag{46}$$

Proof. Let $w = \frac{u_h^{n+1} + u_h^n}{2}$ in (30, iii). Simplifying, we obtain

$$\begin{aligned} &\frac{1}{2c^2 \Delta t} \left(\left\| u_h^{n+1} \right\|^2 - \left\| u_h^n \right\|^2 \right) + \int_\Omega \mathbf{p}_h^{n+1/2} \cdot \nabla \left(\frac{u_h^{n+1} + u_h^n}{2} \right) \mathrm{d}x \\ &\quad = -\frac{1}{c} \int_\Gamma \left| \frac{u_h^{n+1} + u_h^n}{2} \right|^2 \mathrm{d}\Gamma - \int_\omega \lambda_h^{n+1} \left(\frac{u_h^{n+1} + u_h^n}{2} \right) \mathrm{d}x. \end{aligned} \tag{47}$$

From (30, ii), we take $\mathbf{q} = \mathbf{p}_h^{n+1/2}$ to get

$$\int_\Omega \frac{\mathbf{p}_h^{n+1/2} - \mathbf{p}_h^{n-1/2}}{\Delta t} \cdot \mathbf{p}_h^{n+1/2} \, \mathrm{d}x - \int_\Omega \nabla u_h^n \cdot \mathbf{p}_h^{n+1/2} \, \mathrm{d}x = 0. \tag{48}$$

Again from (30, ii) replacing n by $n + 1$ and $\mathbf{q} = \mathbf{p}_h^{n+1/2}$ we get

$$\int_\Omega \frac{\mathbf{p}_h^{n+3/2} - \mathbf{p}_h^{n+1/2}}{\Delta t} \cdot \mathbf{p}_h^{n+1/2} \, \mathrm{d}x - \int_\Omega \nabla u_h^{n+1} \cdot \mathbf{p}_h^{n+1/2} \, \mathrm{d}x = 0. \tag{49}$$

Adding Eqs. (48) and (49) and substituting the result in (47) we have

$$\frac{1}{2\Delta t}\left\{\frac{1}{c^2}\left(\left\|u_h^{n+1}\right\|^2-\left\|u_h^{n}\right\|^2\right)+\left(\mathbf{p}_h^{n+3/2},\mathbf{p}_h^{n+1/2}\right)-\left(\mathbf{p}_h^{n+1/2},\mathbf{p}_h^{n-1/2}\right)\right\}$$
$$=-\frac{1}{c}\int_\Gamma\left|\frac{u_h^{n+1}+u_h^{n}}{2}\right|^2\mathrm{d}\Gamma-\int_\omega\lambda_h^{n+1}\left(\frac{u_h^{n+1}+u_h^{n}}{2}\right)\mathrm{d}x. \tag{50}$$

Next, from (30, iv) by taking $\mu_h=\lambda_h^{n+1}$, and also $\mu_h=\lambda_h^{n+2}$ we have, respectively

$$\int_\omega\lambda_h^{n+1}u_h^{n+1}\,\mathrm{d}x=0\quad\text{and}\quad\int_\omega\lambda_h^{n+2}u_h^{n+1}\,\mathrm{d}x=0. \tag{51}$$

This implies that

$$\int_\omega\lambda_h^{n+1}\left(\frac{u_h^{n}+u_h^{n+1}}{2}\right)\mathrm{d}x=0. \tag{52}$$

Using the parallelogram law we can write

$$\left(\mathbf{p}_h^{n+3/2},\mathbf{p}_h^{n+1/2}\right)=\frac{1}{4}\left\|\mathbf{p}_h^{n+3/2}+\mathbf{p}_h^{n+1/2}\right\|^2-\frac{1}{4}\left\|\mathbf{p}_h^{n+3/2}-\mathbf{p}_h^{n+1/2}\right\|^2. \tag{53}$$

Similarly

$$\left(\mathbf{p}_h^{n+1/2},\mathbf{p}_h^{n-1/2}\right)=\frac{1}{4}\left\|\mathbf{p}_h^{n+1/2}+\mathbf{p}_h^{n-1/2}\right\|^2-\frac{1}{4}\left\|\mathbf{p}_h^{n+1/2}-\mathbf{p}_h^{n-1/2}\right\|^2. \tag{54}$$

From (30, ii), since $\nabla V_h\subset\mathbf{P}_h$, we have with $n=n$ and $n=n+1$, respectively

$$\mathbf{p}_h^{n+1/2}-\mathbf{p}_h^{n-1/2}=\Delta t\nabla u_h^{n};\quad\mathbf{p}_h^{n+3/2}-\mathbf{p}_h^{n+1/2}=\Delta t\nabla u_h^{n+1}. \tag{55}$$

Substituting (52)–(55) in (50) and using the definition of the operator $\mathscr{S}_h$ we obtain (45). Thus, as in the previous theorem: under the given CFL condition the operator $\mathscr{S}_h$ defines a positive quadratic form, and the CFL condition assures the stability of the scheme (30). □

7. An operator splitting scheme with mixed finite elements for the numerical solution of the wave problem

In this section, we describe a symmetrized operator splitting scheme for the numerical solution of the wave problem (3). The idea behind operator splitting, in the case of the scattering problem, is to decouple the operator that propagates the wave from the operator that enforces the Dirichlet condition on the boundary of the obstacle ω. On a time interval of length Δt, we can construct a two-step splitting scheme by separating the solution of (3) into two steps (subproblems). In one step of time length Δt we will propagate the wave, i.e., solve the wave equation in the whole domain Ω, and in the second step of length Δt we will enforce the Dirichlet condition on $\partial\omega$. The communication between the two steps is via the initial condition. The solution of one subproblem is input as initial conditions to the next subproblem.

The two-step schemes are usually first-order accurate in time, where as a symmetrized version of such schemes gives second-order temporal accuracy, even if the sub-operators involved do not commute [29]. Thus, in order to obtain second-order accurate schemes in time we will construct a (Strang) symmetrization of the two-step scheme outlined above. We can do so in two ways. We perform one of the two steps mentioned above on two intervals of length $\Delta t/2$ separated by the other step performed on an interval of length Δt. This gives rise to two different symmetrized operator splitting schemes.

1. Symmetrized scheme 1:
   - Propagate the wave on an interval of length $\Delta t/2$.
   - Enforce the Dirichlet condition on $\partial\omega$ on an interval of length Δt.
   - Propagate the wave on an interval of length $\Delta t/2$.
2. Symmetrized scheme 2:
   - Enforce the Dirichlet condition on $\partial\omega$ on an interval of length $\Delta t/2$.
   - Propagate the wave on an interval of length Δt.
   - Enforce the Dirichlet condition on $\partial\omega$ on an interval of length $\Delta t/2$.

Again, the communication between the different subproblems of either scheme is via the initial conditions as explained above. The main advantage of operator splitting is that each individual subproblem involves a single operator and is trivial to solve. Also, we can use different discretizations for the numerical implementation of the different subproblems. In [19,20], we have used the fully conforming approach of Section 4 to discretize the subproblems responsible for enforcing the Dirichlet condition on $\bar{\omega}$, and the mixed finite element approach for wave propagation. In this paper, we will use the mixed finite element approach for all the subproblems. In this section, we will demonstrate the numerical implementation of scheme 2. This operator splitting scheme is based on the mixed formulation (30).

Let us define χ_ω to be the characteristic function of the domain ω. On the interval (t^n, t^{n+1}), given $(\phi_h^n, u_h^n, \mathbf{p}_h^n)$, we solve three subproblems to obtain $(\phi_h^{n+1}, u_h^{n+1}, \mathbf{p}_h^{n+1})$ as follows.

• **Operator splitting scheme** SFDDM:

For $n = 0, 1, 2, \ldots, N-1$, solve:

• SUBPROBLEM $(1)_m$: Find $(\phi_h^{n+1/2}, u_h^{n+1/2}, \mathbf{p}_h^{n+1/2}, \lambda_h^{n+1/2})$ such that

$$\begin{aligned}
&\phi_h^{n+1/2} = \phi_h^n,\\
&\mathbf{p}_h^{n+1/2} = \mathbf{p}_h^n,\\
&\frac{1}{c^2}\int_\Omega \frac{u_h^{n+1/2} - u_h^n}{\Delta t/2} w_h \,\mathrm{d}x + \int_\omega \lambda_h^{n+1/2} w_h \,\mathrm{d}\omega = 0 \quad \forall w_h \in \mathbf{V}_h,\\
&\int_\omega \left(u_h^{n+1/2} - \frac{\partial g^{n+1/2}}{\partial t}\right)\mu_h \,\mathrm{d}\omega = 0 \quad \forall \mu_h \in \mathbf{\Lambda}_h.
\end{aligned} \tag{56}$$

• SUBPROBLEM $(2)_m$: Find $(\tilde{\phi}_h^{n+1}, \tilde{u}_h^{n+1}, \tilde{\mathbf{p}}_h^{n+1})$ such that

$$\begin{aligned}
&\frac{\tilde{\phi}_h^{n+1} - \phi_h^{n+1/2}}{\Delta t} = u_h^n,\\
&\int_\Omega \frac{\tilde{\mathbf{p}}_h^{n+1} - \mathbf{p}_h^{n+1/2}}{\Delta t}\mathbf{q}_h \,\mathrm{d}x - \int_\Omega \mathbf{q}\cdot\nabla u_h^{n+1/2}\,\mathrm{d}x = 0 \quad \forall \mathbf{q}_h \in \mathbf{P}_h,\\
&\frac{1}{c^2}\int_\Omega \frac{\tilde{u}_h^{n+1} - u_h^{n+1/2}}{\Delta t} w_h \,\mathrm{d}x + \int_\Omega \tilde{\mathbf{p}}_h^{n+1}\cdot\nabla w_h \,\mathrm{d}x + \frac{1}{c}\int_\Gamma \frac{\tilde{u}_h^{n+1} + u_h^{n+1/2}}{2} w_h \,\mathrm{d}\Gamma = 0 \quad \forall w_h \in \mathbf{V}_h.
\end{aligned} \tag{57}$$

• SUBPROBLEM $(3)_m$: Find $(\phi_h^{n+1}, u_h^{n+1}, \mathbf{p}_h^{n+1}, \lambda_h^{n+1})$ such that

$$\begin{aligned}
&\phi_h^{n+1} = \tilde{\phi}_h^{n+1},\\
&\mathbf{p}_h^{n+1} = \tilde{\mathbf{p}}_h^{n+1},\\
&\frac{1}{c^2}\int_\Omega \frac{u_h^{n+1} - \tilde{u}_h^{n+1}}{\Delta t/2} w_h \,\mathrm{d}x + \int_\omega \lambda_h^{n+1} w_h \,\mathrm{d}\omega = 0 \quad \forall w_h \in \mathbf{V}_h,\\
&\int_\omega \left(u_h^{n+1} - \frac{\partial g^{n+1}}{\partial t}\right)\mu_h \,\mathrm{d}\omega = 0 \quad \forall \mu_h \in \mathbf{\Lambda}_h.
\end{aligned} \tag{58}$$

Subproblems $(1)_m$ and $(3)_m$ enforce the Dirichlet boundary condition on $\bar{\omega}$, each on an interval of length $\Delta t/2$. In both these steps ϕ and $\mathbf{p}$ are kept constant. Subproblem $(2)_m$ is pure wave propagation. The Dirichlet boundary condition is absent in this step. In the scheme presented above, we have retained a first-order absorbing boundary condition in subproblem $(2)_m$. We will replace this subproblem with one that uses perfectly matched layers, which are developed in Section 8, to perform numerical experiments in Section 9.

8. Construction of a PML model in 2D

In this section, we construct a PML model to replace the first-order absorbing boundary condition Eq. (3, iii). We will start with a first-order system defined in the space $\Omega = [-\infty, 0]^2$, and we will construct a PML model in the positive half space in $\mathbb{R}^2$. The construction of the PML is based on a change of variables approach in the complex plane that was used in [30] for constructing PML's for Maxwell's equations. The construction in this section is closely related to that in [31]. In this and succeeding sections, we have used ρ to denote the frequency as ω denotes the scattering obstacle. Consider the scalar wave equation in Ω written as a system of first-order equations

$$\begin{aligned} &\text{(i)} && \frac{1}{c^2}\frac{\partial u}{\partial t} - \nabla \cdot \mathbf{p} = 0, \\ &\text{(ii)} && \frac{\partial \mathbf{p}}{\partial t} - \nabla u = 0. \end{aligned} \tag{59}$$

Applying the Fourier transform to (59, i) and (59, ii) (replace $\frac{\partial}{\partial t}$ by $-\mathrm{i}\rho$), we have

$$\begin{aligned} &\text{(i)} && \frac{-\mathrm{i}\rho}{c^2}\hat{u} - \nabla \cdot \hat{\mathbf{p}} = 0, \\ &\text{(ii)} && -\mathrm{i}\rho\hat{\mathbf{p}} - \nabla\hat{u} = 0. \end{aligned} \tag{60}$$

Here, $\hat{w}$ is the Fourier transform of w for all field variables w. With $\hat{\mathbf{p}} = (\hat{p}_x, \hat{p}_y)^{\mathrm{T}}$ we will rewrite (60) in scalar form as

$$\begin{aligned} &\text{(i)} && \frac{-\mathrm{i}\rho}{c^2}\hat{u} - \frac{\partial \hat{p}_x}{\partial x} - \frac{\partial \hat{p}_y}{\partial y} = 0, \\ &\text{(ii)} && -\mathrm{i}\rho\hat{p}_x - \frac{\partial \hat{u}}{\partial x} = 0, \\ &\text{(iii)} && -\mathrm{i}\rho\hat{p}_y - \frac{\partial \hat{u}}{\partial y} = 0. \end{aligned} \tag{61}$$

Next, we construct the change of variables

$$\tilde{x} = \begin{cases} x, & x < 0, \\ x + \frac{\mathrm{i}}{\rho}\int_0^x \sigma_x(s)\,\mathrm{d}s, & \text{otherwise}, \end{cases} \tag{62}$$

and

$$\tilde{y} = \begin{cases} y, & y < 0, \\ y + \frac{\mathrm{i}}{\rho}\int_0^y \sigma_y(s)\,\mathrm{d}s, & \text{otherwise}, \end{cases} \tag{63}$$

with $\sigma_x(0) = \sigma_y(0) = 0$. Using (62) and (63), we extend the first-order system in (61) to the complex plane as

$$\begin{aligned}
&\text{(i)} && \frac{-\mathrm{i}\rho}{c^2}\hat{u} - \frac{\partial \hat{p}_x}{\partial \tilde{x}} - \frac{\partial \hat{p}_y}{\partial \tilde{y}} = 0,\\
&\text{(ii)} && -\mathrm{i}\rho\hat{p}_x - \frac{\partial \hat{u}}{\partial \tilde{x}} = 0,\\
&\text{(iii)} && -\mathrm{i}\rho\hat{p}_y - \frac{\partial \hat{u}}{\partial \tilde{y}} = 0.
\end{aligned} \tag{64}$$

Next, we use the chain rule to replace the derivatives in $\tilde{x},\ \tilde{y}$ by derivatives in x, y as follows. We have for $x > 0$, $y > 0$, respectively

$$\frac{\mathrm{d}x}{\mathrm{d}\tilde{x}} = \frac{1}{1 + (\mathrm{i}\sigma_x)/\rho}; \quad \frac{\mathrm{d}y}{\mathrm{d}\tilde{y}} = \frac{1}{1 + (\mathrm{i}\sigma_y)/\rho}. \tag{65}$$

Thus, from (64) and (65) we have

$$\begin{aligned}
&\text{(i)} && \frac{-\mathrm{i}\rho}{c^2}\hat{u} - \frac{1}{1 + (\mathrm{i}\sigma_x)/\rho}\frac{\partial \hat{p}_x}{\partial x} - \frac{1}{1 + (\mathrm{i}\sigma_y)/\rho}\frac{\partial \hat{p}_y}{\partial y} = 0,\\
&\text{(ii)} && -\mathrm{i}\rho\hat{p}_x - \frac{1}{1 + (\mathrm{i}\sigma_x)/\rho}\frac{\partial \hat{u}}{\partial x} = 0,\\
&\text{(iii)} && -\mathrm{i}\rho\hat{p}_y - \frac{1}{1 + (\mathrm{i}\sigma_y)/\rho}\frac{\partial \hat{u}}{\partial y} = 0.
\end{aligned} \tag{66}$$

Next, we define the variables

$$\begin{aligned}
&\text{(i)} && \tilde{p}_x = \big(1 + (\mathrm{i}\sigma_y)/\rho\big)\hat{p}_x,\\
&\text{(ii)} && \tilde{p}_y = (1 + (\mathrm{i}\sigma_x)/\rho)\hat{p}_y,\\
&\text{(iii)} && \hat{v} = \big(1 + (\mathrm{i}\sigma_y)/\rho\big)\hat{u},\\
&\text{(iv)} && \hat{q}_x = \frac{1}{1 + (\mathrm{i}\sigma_y)/\rho}\tilde{p}_x,\\
&\text{(v)} && \hat{q}_y = \frac{1}{1 + (\mathrm{i}\sigma_x)/\rho}\tilde{p}_y.
\end{aligned} \tag{67}$$

We use $\mathbf{p}$ to be the inverse Fourier transform of $\tilde{\mathbf{p}}$ as $\hat{\mathbf{p}}$ coincides with $\tilde{\mathbf{p}}$ in the domain Ω. Let $\mathbf{q} = (q_x, q_y)^{\mathrm{T}}$ and define

$$S_{xy} = \begin{pmatrix} \sigma_x & 0 \\ 0 & \sigma_y \end{pmatrix}; \quad S_{yx} = \begin{pmatrix} \sigma_y & 0 \\ 0 & \sigma_x \end{pmatrix}. \tag{68}$$

Using the above definitions and taking the inverse Fourier transform of the resulting equations (replace $-\mathrm{i}\rho$ by $\partial/\partial t$), we obtain a two-dimensional PML model for the wave equation in the time domain as

$$\begin{aligned}
&\text{(i)} && \frac{\partial \mathbf{q}}{\partial t} + S_{xy}\mathbf{q} = \nabla u,\\
&\text{(ii)} && \frac{\partial \mathbf{p}}{\partial t} = \frac{\partial \mathbf{q}}{\partial t} + S_{yx}\mathbf{q},\\
&\text{(iii)} && \frac{\partial v}{\partial t} + \sigma_x v - c^2\nabla\cdot\mathbf{p} = 0,\\
&\text{(iv)} && \frac{\partial u}{\partial t} + \sigma_y u = \frac{\partial v}{\partial t},
\end{aligned} \tag{69}$$

in which we must solve for $(u, v, \mathbf{p}, \mathbf{q})$. Our PML formulation is different from the system constructed in [31] as we retain a first-order system of equations. Thus, we have to solve for the variables $\mathbf{q}$, $\mathbf{p}$, v and u in the PML system. As in [31] we use the definition of σ_l, $l = 1, 2$ as

$$\sigma_l = \begin{cases} 0 & \text{if} \quad x \leqslant 0, \\ \sigma_{\max}\left(\frac{x}{\delta}\right)^2 & \text{if} \quad x > 0, \end{cases} \tag{70}$$

where $\sigma_{\max} = \frac{3c}{2\delta}\log(R)$, δ being the thickness of the PML, c the speed of propagation, and $R = 10^3$. We have used PML's which are one wavelength thick in our numerical experiments.

8.1. A variational formulation of the PML system

We construct a variational formulation of the time dependent PML system (69) on similar lines as was done for (7).

Find $\{v(t), u(t), \mathbf{q}(t), \mathbf{p}(t)\} \in H_0^1(\Omega) \times H_0^1(\Omega) \times [L^2(\Omega)]^2 \times [L^2(\Omega)]^2$ such that:

$$\begin{aligned}
&\text{(i)} && \int_\Omega \frac{\partial \mathbf{q}}{\partial t} \cdot \mathbf{r}\,dx + \int_\Omega S_{xy}\mathbf{q} \cdot \mathbf{r}\,dx = \int_\Omega \nabla u \cdot \mathbf{r}\,dx \quad \forall \mathbf{r} \in [L^2(\Omega)]^2, \\
&\text{(ii)} && \int_\Omega \frac{\partial \mathbf{p}}{\partial t} \cdot \mathbf{r}\,dx = \int_\Omega \frac{\partial \mathbf{q}}{\partial t} \cdot \mathbf{r}\,dx + \int_\Omega S_{yx}\mathbf{q} \cdot \mathbf{r}\,dx \quad \forall \mathbf{r} \in [L^2(\Omega)]^2, \\
&\text{(iii)} && \int_\Omega \frac{\partial v}{\partial t} w\,dx + \int_\omega \sigma_x v w\,dx + c^2 \int_\Omega \nabla w \cdot \mathbf{p}\,dx = 0 \quad \forall w \in H_0^1(\Omega), \\
&\text{(iv)} && \int_\Omega \frac{\partial u}{\partial t} w\,dx + \int_\Omega \sigma_y u w\,dx = \int_\Omega \frac{\partial v}{\partial t} w\,dx \quad \forall w \in H_0^1(\Omega).
\end{aligned} \tag{71}$$

The discrete formulation of (71) uses the mixed finite element approach of Section 4. The degrees of freedom for $\mathbf{p}_h$ and $\mathbf{q}_h$ are at the midpoints of edges, whereas the degrees of freedom for u_h are v_h are at the vertices of the rectangular elements as shown in Fig. 4. We use central differences in time with the degrees of freedom staggered in time (and space) as before. We note that the PML is terminated by the Dirichlet condition $u = 0$. The first-order system along with the first-order absorbing boundary condition in SUB-PROBLEM $(2)_m$ in the operator spitting scheme SFDDM of Section 7 is replaced by a discrete version of the PML formulation (71).

9. Numerical examples

9.1. Scattering by a disk

We consider the scattering of the harmonic planar waves $e^{-i(\rho t - \mathbf{k}\cdot\mathbf{x})}$ by a perfectly reflecting disk whose radius is 0.25 m. The disc is located at the center of the domain $[0, 3.5] \times [0, 3.5]$. The frequency f is 0.6 GHz, and the wavelength L is 0.5 m. The wavenumber is denoted by $\mathbf{k} = (k_x, k_y)$. The angular frequency is $\rho = 2\pi f$. The wave illuminates ω from the left and propagates horizontally. The distance from the disk to the absorbing boundary is three wavelengths. We have used a rectangular mesh consisting of 113×113 nodes, with the mesh step size $h = 0.5/16$ m. The time step is $\Delta t = 2\pi/(25\rho)$. Thus, the Courant number is $(c\Delta t)/h = 0.64 < 1/\sqrt{2}$. In all our experiments we have kept the mesh ratio to be 2. For this test problem the exact solution is known when Γ is located at infinity. Let the circle be centered at the origin, with radius r_0. The analytic solution for the Dirichlet problem is given by

$$\phi(r,\theta) = -\sum_{n\in\mathbb{Z}} \mathrm{i}^{|n|} J_{|n|}(\rho r_0)\, \mathrm{e}^{\mathrm{i}n\theta} \frac{H_n^{(1)}(\rho r)}{H_n^{(1)}(\rho r_0)} \quad \forall r \in [r_0,\infty),\ \ \forall\theta\in[0,2\pi], \tag{72}$$

where $H_n^{(1)}$ is the *Hankel* function of the first kind and J_n is the *Bessel* function of order n.

We present plots of the real part of the exact solution (72), and the real part of the solution computed using the operator splitting scheme of Section 7, with the PML model of Section 8, for the problem of scattering by a disk. The computed solution is time integrated for 175 time steps, i.e., until $t = 7L/c = 7/f$. In Fig. 5, a full view of the exact solution and the computed solution for a discretization with 16 nodes per wavelength is presented. The figures show a remarkable agreement, considering that the mesh is not locally modified to fit $\partial\omega$, as some other fictitious domain methods do. Fig. 6 presents the error, with respect to the exact solution at points on the line $x = 1.75$ (left), and with respect to the exact solution at points on the line $y = 1.75$ (right). In both cases the error seems to be decreasing as $\mathcal{O}(h)$.

We calculate the relative error (RE) of our computed solution ϕ_C, with respect to the exact solution ϕ_E, where

$$\mathrm{RE} = \frac{\|\phi_C - \phi_E\|_{L^2(\Omega)}}{\|\phi_E\|_{L^2(\Omega)}}. \tag{73}$$

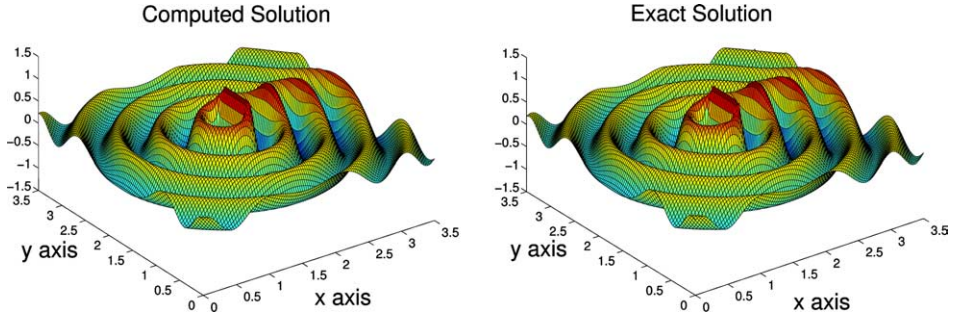

Fig. 5. Real parts of the exact solution (right) and the solution computed with the operator splitting scheme (left).

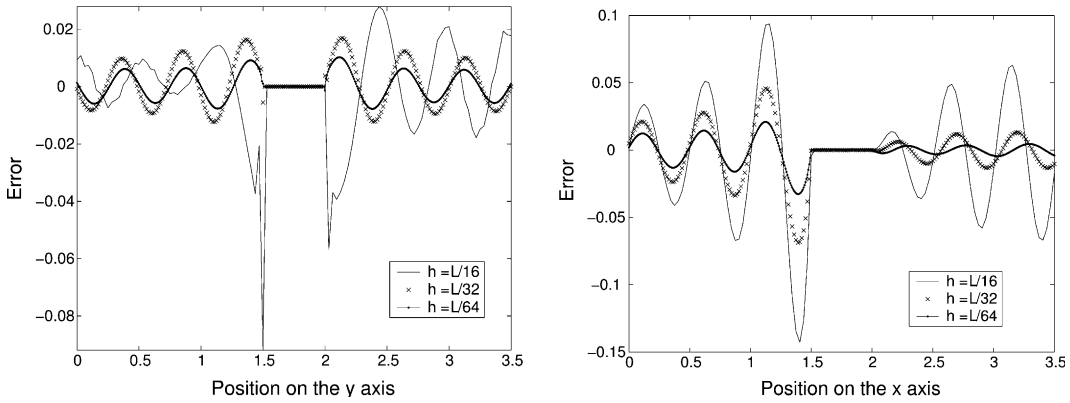

Fig. 6. Error in the real parts of the computed solutions on the half-line containing the center of ω and parallel (right), respectively, perpendicular (left) to the incidence direction for different values of h.

In Table 1, we present relative errors for different discretizations, for the operator splitting scheme SFDDM of Section 7 combined with the PML of Section 8, and the mixed finite element scheme (MDM) of Section 4 combined with the PML of Section 8. As can be seen from Table 1, both methods introduce the same relative errors. Thus, the operator splitting does not seem to produce any additional error. The ratios of errors for successive discretizations starts out to be 4 for both schemes. But asymptotically these ratios approach 2 indicating $\mathcal{O}(h)$ spatial accuracy of both schemes.

We have not presented results for the fully conforming approach of Section 3 as one cannot see any convergence to the exact solution for this scheme. The ratios between relative errors for successive discretizations is between 1 and 2 for this case. In [19], we have shown that this is due to the first-order absorbing boundary condition that is used in the fully conforming approach.

9.2. Scattering by multiple disks

We consider the scattering of the harmonic planar waves $e^{-i(\rho t - \mathbf{k}\cdot\mathbf{x})}$ by nine perfectly reflecting disks whose radius is 0.25 m on the domain $\Omega = [0,5]\times[0,5]$. The frequency is 0.6 GHz, and the wavelength is 0.5 m. The wave illuminates ω from the left and propagates horizontally. We have used a rectangular mesh consisting of 321×321 nodes, with the mesh step size $h = 0.5/32$ m. The time step is $\Delta t = 2\pi/(50\rho)$.

For this test problem the exact solution is not known. We compare our results obtained using the operator splitting scheme, with a reference solution that is obtained by solving a time harmonic problem in which the mesh is locally fitted to the boundary of the obstacles [32] leading to $\mathcal{O}(h^2)$ accurate discretizations.

The details of the computational domain are shown in Fig. 7. Each disk is one wavelength in diameter. The distance between two neighboring disks is one wavelength in the x, and/or y direction. We have kept the (artificial) boundary Γ at least two and a half wavelengths from each disk. In Fig. 8 (left), we present a contour plot of the solution at 2000 time steps. We see a very good comparison with the reference solution shown in Fig. 8 (right). However, the convergence of our solution to the time harmonic solution is slow because of the presence of multiple obstacles (a non-convex obstacle); nonetheless, our solution compares very well with the time harmonic solution. In Fig. 9, we compare a slice of the two solutions which is perpendicular (right), respectively, parallel (left) to the direction of propagation of the wave. In each case the comparison is shown at 2000 time steps. The figures demonstrate the convergence of our solution to the time harmonic reference solution. In Fig. 10, we provide a comparison of the time evolution of the computed solution with the reference solution for 2000 time steps at the point (1.5, 2). We calculate the time evolution for the time harmonic solution $U(x,y)$ by multiplying it with $e^{-i\rho t}$, and considering the real part of this product, i.e., $\mathrm{Re}(U(x,y)e^{-i\rho t})$. Again, this figure demonstrates the convergence of our solution to the time harmonic reference solution.

For all the cases presented above the number of iterations needed for convergence in the conjugate gradient (Uzawa) algorithm of Section 5 were between 11 and 16 for all values of h and Δt.

Table 1
Relative errors for different discretizations for the operator splitting scheme (SFDDM) of Section 7 and the mixed finite element scheme (MDM) of Section 4

N	L/h	SFDDM		MDM	
		Error	Ratio	Error	Ratio
113^2	16	1.242e − 1		1.235e − 1	
225^2	32	2.944e − 2	4.22	2.910e − 2	4.24
449^2	64	8.727e − 3	3.37	8.626e − 3	3.37
897^2	128	3.899e − 3	2.24	3.901e − 3	2.21

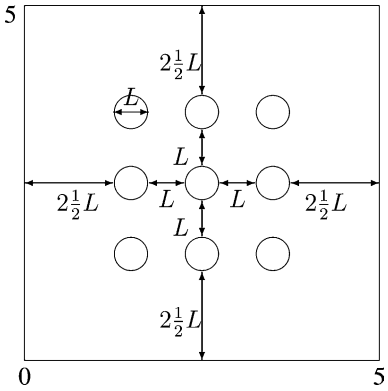

Fig. 7. Domain Ω with nine disks.

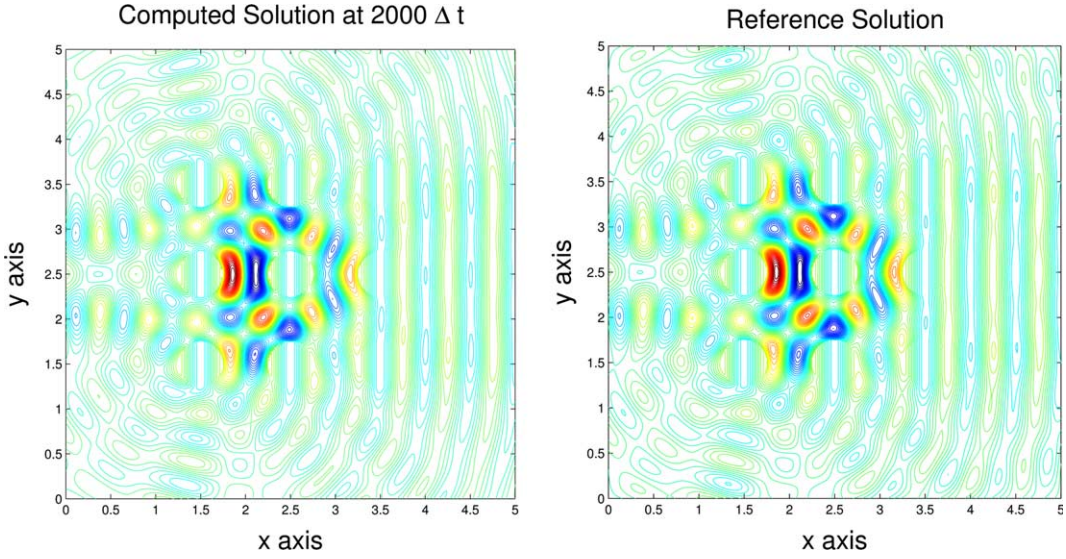

Fig. 8. Contour plots of the computed solution after 2000 time steps (left) and the reference solution (right).

10. A 1D plane wave analysis

In this section, we analyze the distributed multiplier based fictitious domain method for a 1D wave problem. Based on this analysis we compare our method with two alternate methods that can be used for the solution of the same problem. The first method is a finite difference scheme which we denote as FDM, that uses central differences in space and time to discretize the problem on a uniform mesh. The second scheme is another fictitious domain method that is based on a boundary Lagrange multiplier which we denote as FDBM. This method was introduced in [13–15].

We consider the 1D wave equation with a Dirichlet boundary condition. The problem is to find Φ such that

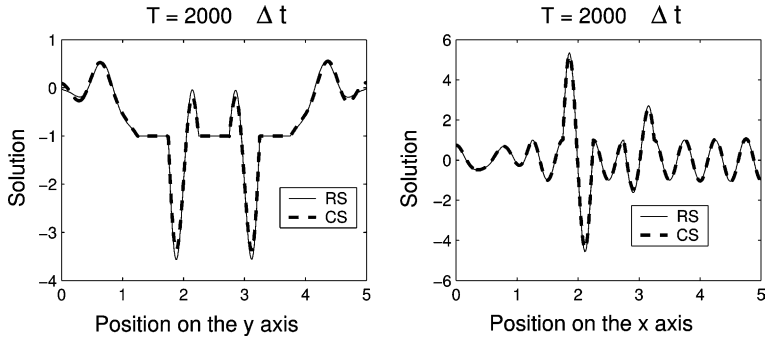

Fig. 9. Slice of the solution on the line $y = 2.5$ (right) and the line $x = 2.5$ (left). RS denotes the reference solution and CS denotes the computed solution.

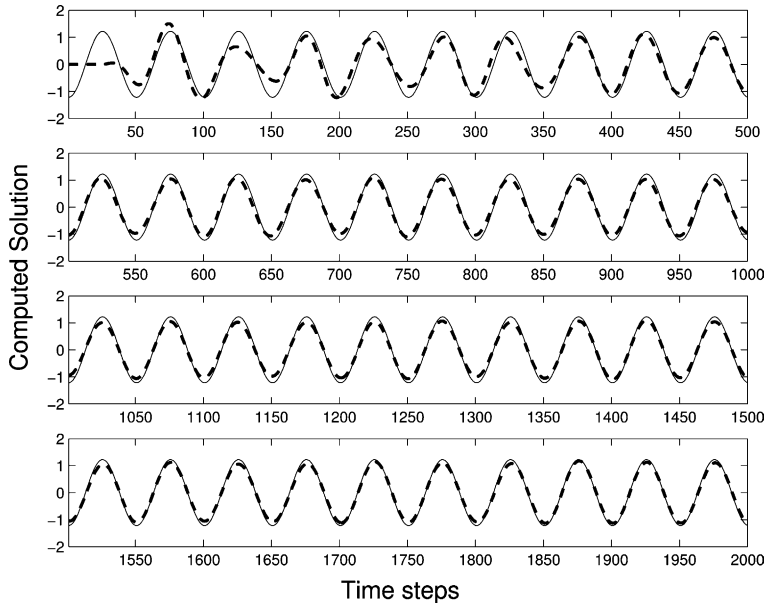

Fig. 10. Comparison of the time evolution of the computed solution (-----) with the reference solution (——) for 2000 time steps at the point (1.5, 2).

$$
\begin{aligned}
&\frac{1}{c^2}\frac{\partial^2 \Phi}{\partial t^2} - \frac{\partial^2 \Phi}{\partial x^2} = 0, \quad x < x_r,\\
&\Phi(x = x_r) = 0,\\
&\Phi(t = 0) = \Phi_0 \in H^1(\mathbb{R}), \quad \Phi_0(x = x_r) = 0,\\
&\frac{\mathrm{d}\Phi}{\mathrm{d}t}(t = 0) = \Phi_1 \in L^2(\mathbb{R}),
\end{aligned}
\tag{74}
$$

where $0 \leqslant x_r < 1$.

As shown in Fig. 11 the domain ω, in our fictitious domain method, for the 1D case is the interval (x_r, ∞). Thus, in our fictitious domain formulation, the problem is extended to the entire real line $\mathbb{R}$,

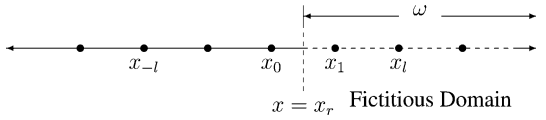

Fig. 11. The fictitious domain.

and the Dirichlet boundary condition, $\phi(x_r) = 0$, is imposed via the introduction of a distributed Lagrange multiplier λ defined over the domain, $\bar{\omega} = [x_r, \infty)$.

We will take $x_r = rh$, with $0 \leqslant r < 1$. Thus, x_r does not coincide with a nodal point unless $r = 0$. We calculate the mass matrix for the discrete problem by using the trapezoidal rule to obtain a scheme that is explicit in time. The discrete scheme for our fictitious domain method can be written as:

Find $(\phi_{h,l}^{n+1}, \lambda_{h,k}^{n+1})$ such that $\forall l \in \mathbb{Z}, \quad k = r$ or $k \in \mathbb{N}, \ k \geqslant 2 : \phi_{h,l}^{n+1} \in \mathbb{R}$ and $\lambda_{h,k}^{n+1} \in \mathbb{R}$

$$\begin{aligned}
&\text{(i)} \quad \frac{\phi_{h,l}^{n+1} - 2\phi_{h,l}^{n} + \phi_{h,l}^{n-1}}{c^2\Delta t^2} - \frac{\phi_{h,l+1}^{n} - 2\phi_{h,l}^{n} + \phi_{h,l-1}^{n}}{h^2} + \lambda_{h,r}^{n+1}((1-r)\delta_{l,0} + r\delta_{l,1}) \\
&\qquad + \sum_{k \geqslant 2, k \in \mathbb{N}} \lambda_{h,k}^{n+1}\delta_{l,k} = 0 \quad \forall l \in \mathbb{Z}, \\
&\text{(ii)} \quad (1-r)\phi_{h,0}^{n+1} + r\phi_{h,1}^{n+1} = 0, \\
&\text{(iii)} \quad \phi_{h,l}^{n+1} = 0 \quad \text{for } l \in \mathbb{N}, \ l \geqslant 2, \\
&\text{(iv)} \quad \phi_{h,l}^{0} = \phi_{0,h,l}, \quad \text{and} \quad \frac{\phi_{h,l}^{1} - \phi_{h,l}^{-1}}{2\Delta t} = \phi_{1,h,l} \quad \forall l \in \mathbb{Z}.
\end{aligned} \tag{75}$$

In the above, $\delta_{l,k}$ is the Kronecker delta function.

We now perform a plane wave analysis of the different schemes outlined above for the numerical solution of the 1D wave problem (74). We will calculate the *reflection coefficient* in each case and compare the different schemes on this basis.

We first note that the 1D wave equation (74) satisfies a solution of the form

$$\phi(x,t) = \mathrm{e}^{-\mathrm{i}\rho t}\left(\mathrm{e}^{-\mathrm{i}k(x-x_r)} + R_{\mathrm{cont}}\,\mathrm{e}^{\mathrm{i}k(x-x_r)}\right). \tag{76}$$

The Dirichlet condition $\phi(x = x_r) = 0$ implies that the reflection coefficient R_{cont} is given by

$$R_{\mathrm{cont}} = -1. \tag{77}$$

The dispersion relation here is given by $\rho = kc$ with c being the speed of propagation and k is the wave number.

In the finite difference scheme (FDM) the Dirichlet boundary condition is moved to the nodal point $x_0 = 0$. We use centered differences in space and time for this scheme. In this scheme we look for a solution of the form

$$\phi_{h,l}^{n} = \mathrm{e}^{-\mathrm{i}\rho n\Delta t}\left(\mathrm{e}^{-\mathrm{i}kh(l-r)} + R_{\mathrm{FDM}}\,\mathrm{e}^{\mathrm{i}kh(l-r)}\right) \quad \text{if } \ l \leqslant 0. \tag{78}$$

This gives the superposition of the incident and the reflected waves in the domain $l \leqslant 0$. Using the condition $\phi_{h,0}^{n} = 0$ in (78), we have

$$R_{\mathrm{FDM}} = -\mathrm{e}^{2\mathrm{i}hkr} = -1 - 2\mathrm{i}hkr + \mathcal{O}(h^2), \tag{79}$$

as a series in h. Thus, if $r = 0$ in (79) then we have $R_{\mathrm{FDM}} = -1 = R_{\mathrm{cont}}$. Otherwise, the numerically reflected wave in the FDM scheme is identical to the reflected wave in the continuous case with a phase error of $2\mathrm{i}hkr$. For the FDM as well as for both the fictitious domain methods to be analyzed below the dispersion relation is given by

$$\sin((\rho\Delta t)/2) = \eta \sin((hk)/2), \tag{80}$$

where $\eta = (c\Delta t)/h$ is the Courant number. If the CFL condition $c\Delta t = h$, i.e., $\eta = 1$ is satisfied then the dispersion relation reduces to that of the continuous case, i.e., $\rho = kc$.

In the case of the fictitious domain method with a distributed multiplier we look for a solution of the form

$$\phi_{h,l}^n = \begin{cases} e^{-i\rho n\Delta t}\left(e^{-ikh(l-r)} + R_{\mathrm{FDDM}}\, e^{ikh(l-r)}\right) & \text{if} \quad l \leqslant 0, \\ T_{\mathrm{FDDM}}\, e^{-i\rho n\Delta t}\, e^{-ikh(l-r)} & \text{if} \quad l = 1, \\ 0 & \text{if} \quad l \geqslant 2, \end{cases} \tag{81}$$

where T_{FDDM} is the transmission coefficient and

$$\lambda_{h,j}^{n+1} = \begin{cases} \lambda_r\, e^{-i\rho n\Delta t} & \text{if} \quad j = r, \\ \lambda_2\, e^{-i\rho n\Delta t} & \text{if} \quad j = 2, \\ 0 & \text{if} \quad j \geqslant 3. \end{cases} \tag{82}$$

For this case the reflection coefficient R_{FDDM} is found to be

$$R_{\mathrm{FDDM}} = \frac{-\xi^{2r}\left((\xi(1-r)+r)^2 + (1-r)^2\right)}{(1-r+\xi r)^2 + \xi^2(1-r)^2}, \tag{83}$$

with $\xi = e^{ikh}$. As a series in h we have

$$R_{\mathrm{FDDM}} = -1 - \frac{2ikr(1-r)(2-r)h}{2-2r+r^2} + \mathcal{O}(h^2). \tag{84}$$

Thus, if $r = 0$ then $R_{\mathrm{FDDM}} = -1$ otherwise we have a first-order accurate reflection coefficient for this scheme. The reflection coefficients in the case of the operator splitting scheme with the distributed multiplier based fictitious domain method are the same as in (83) and (84).

Finally, we consider a fictitious domain method which utilizes a boundary multiplier. This method was analyzed in [14,15]. We present here the relevant results. In this case the Dirichlet boundary condition is imposed at the point x_r via the introduction of a (boundary) Lagrange multiplier. We can obtain the discrete scheme for this method from the discrete scheme for the distributed multiplier fictitious domain method by dropping the Lagrange multiplier terms corresponding to the nodal points x_j, $j \geqslant 2$ in (75, i), and by dropping the Eq. (75, iii). We look for a solution of the form

$$\phi_{h,l}^n = \begin{cases} e^{-i\rho n\Delta t}\left(e^{-ikh(l-r)} + R_{\mathrm{FDBM}}\, e^{ikh(l-r)}\right) & \text{if} \quad l \leqslant 0, \\ T_{\mathrm{FDBM}}\, e^{-i\rho n\Delta t}\, e^{-ikh(l-r)} & \text{if} \quad l \geqslant 1, \end{cases} \tag{85}$$

and

$$\lambda_{h,r}^{n+1} = \lambda_r\, e^{-i\rho n\Delta t}. \tag{86}$$

The reflection coefficient R_{FDBM} is given by

$$R_{\mathrm{FDBM}} = \frac{-\xi^{2r-1}(\xi(1-r)+r)^2}{\xi + 2r(1-r)(1-\xi)}. \tag{87}$$

As a series in h, we have

$$R_{\mathrm{FDBM}} = -1 - 2ikr(1-r)h + \mathcal{O}(h^2). \tag{88}$$

Again, we notice that if $r = 0$, then from (87) we have $R = -1 = R_{\mathrm{cont}}$ as in the case of the scheme FDDM. Comparing the series expansions (88) with (84), we see that the distributed multiplier scheme has an extra

factor of $(2-r)/(2-2r+r^2)$ in the $\mathcal{O}(h)$ term for the expression for R_{FDDM} as compared to the expression for R_{FDBM}. So the distributed multiplier method produces an error in the reflection coefficient that is greater than the corresponding coefficient for the boundary multiplier case. This is due to the fact that in the FDDM the entire wave is reflected back from the Lagrange multipliers interior to the obstacle ω, whereas in the boundary multiplier case a part of the wave is transmitted through ω. We have

$$\frac{2-r}{2-2r+r^2} = 1 + \frac{r(1-r)}{2-2r+r^2} \leqslant 1.2071 \quad \text{for } 0 \leqslant r < 1, \tag{89}$$

where the maximum value occurs at $r = 0.5858$.

We now compare the three different schemes FDM, FDDM, and FDBM, on the basis of their reflection coefficients. Fig. 12 plots the error in the amplitude of the reflected wave

$$|R| - |R_{\mathrm{cont}}| = |R| - 1, \tag{90}$$

against the number of nodes per wavelength L/h (left), for $r = 0.5$, where L denotes the wavelength, and against r (right) for $L/h = 20$. We observe from Fig. 12 that for both the FDM and the FDDM schemes, the entire wave is reflected back into the domain $(-\infty, x_r)$, albeit with different phase errors as shown in Fig. 13. However, in the case of the scheme FDBM, part of the wave is transmitted through the boundary into the fictitious domain ω.

Thus, the solutions provided by the finite difference scheme and the distributed multiplier based fictitious domain scheme are physically correct solutions, where as there is a non-physical solution that exists inside the fictitious domain ω in the boundary multiplier based fictitious domain method.

In Fig. 13, we plot the phase error $\mathrm{Im}(R)$ in the reflected wave i.e., we plot the imaginary part of the reflection coefficient R against the number of nodes per wavelength for $r = 0.5$ (left), and against r for $L/h = 20$ (right). All three schemes reflect part or the whole wave back with different phase errors. In this case, we see that the phase error is the largest for the finite difference scheme FDM.

Finally, in Fig. 14 we plot the total error in the reflection coefficient

$$\text{Total error} = |R_{\mathrm{cont}} - R| = |-1 - R|, \tag{91}$$

against r for 20 nodes per wavelength (right) and against L/h for $r = 0.5$ (left). The total error is the largest for the finite difference scheme FDM but decreases as $r \to 0$. The error for all schemes becomes comparable as we increase the number of nodes per wavelength.

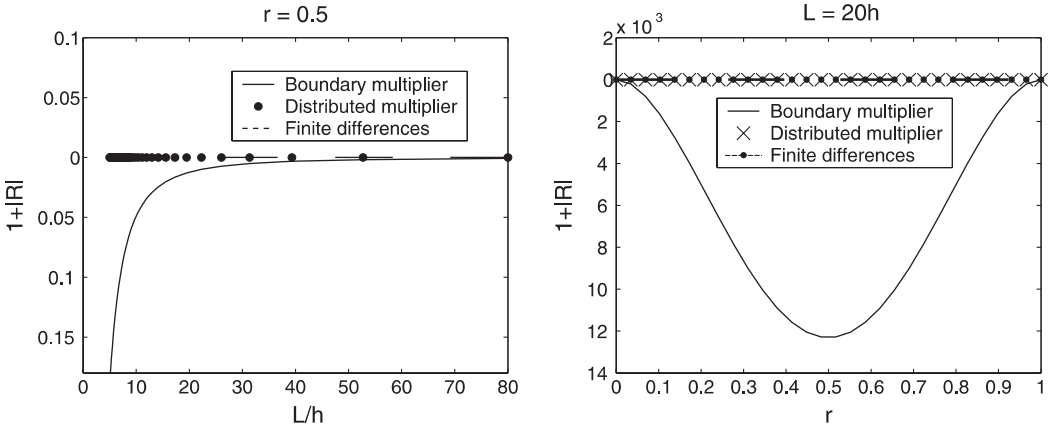

Fig. 12. Error in the amplitude of the reflected wave versus the number of nodes per wavelength (left) for $r = 0.5$, and the error in the amplitude versus r for 20 nodes per wavelength (right).

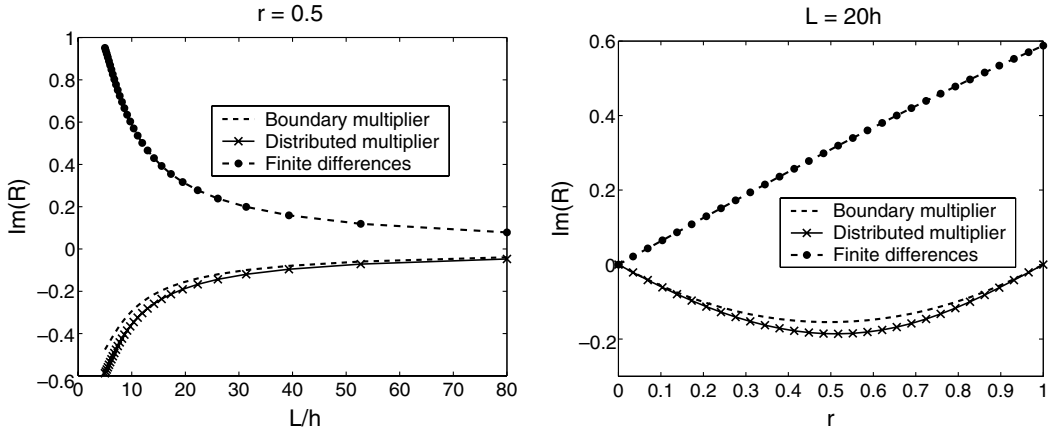

Fig. 13. The phase error in the reflected wave versus the number of nodes per wavelength for $r = 0.5$ (left), and the phase error in the reflected wave versus r for 20 nodes per wavelength (right).

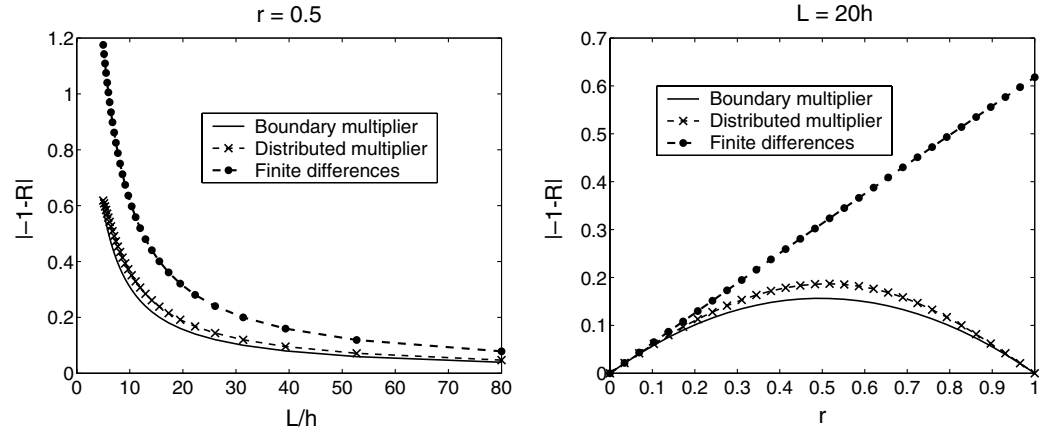

Fig. 14. Total error in the reflection coefficient versus number of nodes per wavelength for $r = 0.5$ (left), and the total error in the reflection coefficient versus r for 20 nodes per wavelength (right).

Remark 1. We finally make the following observation. As seen from (82), most of the Lagrange multipliers are zero except the one on the boundary (i.e., at $x = x_r$) and another one to its right (i.e., at $x = x_2$). Analogously it may be possible to determine, *a priori*, in two and three dimensions the locations of zero and non-zero Lagrange multipliers. This information can then be used to reduce the computational cost.

11. Conclusions and future work

In this paper, we have presented a distributed Lagrange multiplier based fictitious domain method for the numerical solution of a time dependent problem of scattering by an obstacle. In this method the solution to the original problem is extended inside the obstacle and an additional variable, called a Lagrange multiplier, is introduced to enforce the Dirichlet condition on the boundary of the obstacle. This *distributed* Lagrange multiplier is defined on the boundary of the obstacle as well as in the interior of the obstacle, as

opposed to a boundary Lagrange multiplier that is defined only on the boundary of the obstacle. We have presented numerical schemes that utilize a fully conforming approach as well as mixed finite elements. The main advantage of the distributed multiplier based fictitious domain method is the use of uniform meshes to discretize the problems considered.

We have also presented an operator splitting scheme that incorporates the distributed multiplier and perfectly matched layers for solving the scattering problem. From the numerical examples and the one-dimensional analysis presented in this paper, we can conclude that the distributed Lagrange multiplier approach together with operator splitting gives a convenient way to treat the Dirichlet boundary condition. The operator splitting scheme does not seem to introduce any additional error as compared to the (non-split) mixed finite element scheme and hence would be an advantageous way to treat more complicated problems which involve more than one operator. Each subproblem involved in the operator splitting scheme is quite simple to solve. Perfectly matched layers fit well in the mixed framework and these layers work well in practice (about a wavelength or two in size). We have demonstrated via numerical examples that the PML model introduced in this paper works well in practice.

As demonstrated in the 1D analysis in Section 10, the distributed multiplier based fictitious domain method is more accurate than the finite difference approach. Even though the method remains first-order accurate with respect to h the error is much better as compared to the staircase approximation of the finite difference scheme. In the case of the boundary multiplier fictitious domain method the total error in the reflection coefficient is also better than the total error in the finite difference method and slightly better than the distributed multiplier method. However, the distributed multiplier approach has desirable properties, as demonstrated by the phase and amplitude errors in the reflection coefficient, that are not shared by the boundary multiplier approach.

The distributed multiplier based fictitious domain method can be extended to three dimensions in a straightforward manner. Based on Remark 1, we conclude that it is possible to make adjustments to the iterative solution of our discrete problem to reduce computational costs. This method can also be extended to Maxwell's equations and is the subject of a forthcoming paper.

The proof of an inf–sup condition related to the distributed multiplier has not been addressed in this paper and this is one area which needs to be dealt with in the future. In general such proofs are non-trivial and difficult to obtain.

Acknowledgements

The authors thank Dr. T.W. Pan, Dr. J. Toivanen, Dr. K. Lipnikov and Dr. N.L. Gibson for useful comments and suggestions. We also thank Dr. H.T. Banks, Dr. Mac Hyman and Dr. Michael Buksas for their support and encouragement of the first author. This material is based on work supported in part by the Department of Energy under Contract Nos. 03891-001-99-4G, 74837-001-03 49, and/or 86192-001-04 49 from the Los Alamos National Laboratory, and in part by the US Air Force office of Scientific Research under Grants AFOSR F49620-01-1-0026 and AFOSR FA9550-04-1-0220.

References

[1] V.K. Saul'ev, Solution of certain boundary-value problems on high-speed computers by thefictitious-domain method, Sibirsk. Mat. Ž. 4 (1963) 912–925.
[2] G.I. Marchuk, Y.A. Kuznetsov, A.M. Matsokin, Fictitious domain and domain decomposition methods, Sov. J. Numer. Anal. Math. Model. 1 (1986) 3–35.
[3] C. Börgers, O.B. Widlund, On finite element domain imbedding methods, SIAM J. Numer. Anal. 27 (1990) 963–978.
[4] S.A. Finogenov, Y.A. Kuznetsov, Two-stage fictitious components method for solving the Dirichlet boundary value problem, Sov. J. Numer. Anal. Math. Model. 3 (1988) 301–323.

[5] M. Dryja, A capacitance matrix method for Dirichlet problem on polygonal region, Numer. Math. 39 (1982) 51–64.
[6] O.G. Ernst, A finite element capacitance matrix method for exterior Hemholtz problems, Numer. Math. 75 (1996) 175–204.
[7] R. Glowinski, T. Hesla, D.D. Joseph, T.W. Pan, J. Périaux, Distributed Lagrange multiplier methods for particulate flows, in: M.-O. Bristeau, G. Etgen, F. Fitzgibbon, J.-L. Lions, J. Périaux, M.F. Wheeler (Eds.), Computational Science for the 21st Century, Wiley, Chichester, 1997, pp. 270–279.
[8] R. Glowinski, T.W. Pan, J. Périaux, A fictitious domain method for Dirichlet problem and applications, Comput. Meth. Appl. Mech. Eng. 111 (1994) 283–303.
[9] Y.A. Kuznetsov, Iterative analysis of finite element problems with Lagrange multipliers, in: M.-O. Bristeau, G. Etgen, F. Fitzgibbon, J.-L. Lions, J. Périaux, M.F. Wheeler (Eds.), Computational Science for the 21st Century, Wiley, Chichester, 1997, pp. 170–178.
[10] R. Glowinski, Y. Kuznetsov, On the solution of the Dirichlet problem for linear elliptic operators by a distributed Lagrange multiplier method, C.R. Acad. Sci. Paris Sér. I Math. 327 (1998) 693–698.
[11] E. Heikkola, T. Rossi, P. Tarvainen, Y. Kuznetsov, Efficient preconditioners based on fictitious domains for elliptic FE-problems with Lagrange multipliers, in: H.G. Bock, F. Brezzi, R. Glowinski, G. Kanschat, Y. Kuznetsov, J. Périaux, R. Rannacher (Eds.), ENUMATH 97, World Scientific, Singapore, 1998, pp. 646–661.
[12] C. Atamian, P. Joly, Une analyse de la méthode des domaines fictifs pour le probleme de Hemholtz extérieur, Tech. Rep. 1378, INRIA, 1991.
[13] M.O. Bristeau, V. Girault, R. Glowinski, T.W. Pan, J. Périaux, Y. Xiang, On a fictitious domain method for flow and wave problems, in: R. Glowinski (Ed.), Domain Decompostition Methods in Sciences and Engineering, Wiley, Chichester, 1997, pp. 361–386.
[14] F. Collino, P. Joly, F. Millot, Fictitious domain method for unsteady problems: application to electromagnetic scattering, J. Comput. Phys. 138 (1997) 907–938.
[15] S. Garces, Une méthode de domaines fictifs pour la modélisation des structures rayonnantes tridimensionnelles, Ph.D. Thesis, Ecole Nationale Supérieure de Aéronautique et de Espace, 1997.
[16] R. Glowinski, T.W. Pan, J. Périaux, A fictitious domain method for external incompressible viscous flow modeled by Navier–Stokes equations, Comput. Math. Appl. Mech. Eng. 112 (1994) 113–148.
[17] C. Atamian, G.V. Dinh, R. Glowinski, J. He, J. Périaux, On some imbedding methods applied to fluid dynamics and electromagnetics, Comput. Meth. Appl. Mech. Eng. 91 (1991) 1271–1299.
[18] J. He, Méthodes de domaines fictifs en méchanique des fluides: Applications aux écoulements potentiels instationnaires autour d'obstacles mobiles, Ph.D. Thesis, Université Paris VI, 1994.
[19] V. Bokil, Computational methods for wave propagation problems in unbounded domains, Ph.D. Thesis, Department of Mathematics, University of Houston, May 2003.
[20] V. Bokil, R. Glowinski, A fictitious domain method with operator splitting for wave problems in mixed form, in: G.C. Cohen, E. Heikkola, P. Joly, P. Neittaanmäki (Eds.), Proceedings of Waves 2003: The Sixth International Conference on Mathematical and Numerical Aspects of Wave Propagation, Springer, Berlin, 2003, pp. 437–442.
[21] V. Girault, R. Glowinski, T.W. Pan, A fictitious-domain method with distributed multiplier for the Stokes problem, C.R. Acad. Sci. Paris Sér. I Math. 327 (1998) 693–698.
[22] R. Glowinski, T.W. Pan, J. Périaux, Distributed Lagrange multiplier methods for incompressible viscous flow around moving rigid bodies, Comput. Meth. Appl. Mech. Eng. 151 (1998) 181–194.
[23] A. Taflove, Computational Electrodynamics: The Finite-Difference Time-Domain Method, Artech House, Norwood, MA, 1995.
[24] A. Taflove, Advances in Computational Electrodynamics: The Finite-Difference Time-Domain Method, Artech House, Norwood, MA, 1998.
[25] V. Girault, R. Glowinski, Error analysis of a fictitious domain method applied to a Dirichlet problem, Jpn. J. Ind. Appl. Math. 12 (3) (1995) 487–514.
[26] F. Kikuchi, Mixed and penalty formulations for finite element analysis of an eigenvalue problem in electromagnetism, Comput. Meth. Appl. Mech. Eng. 64 (1-3) (1987) 509–521.
[27] R. Glowinski, P. LeTallec, Augmented Lagrangian and Operator Splitting Methods in Nonlinear Mechanics, SIAM, Philadelphia, PA, 1989.
[28] G.I. Marchuk, Splitting and alternating direction methods, in: P.G. Ciarlet, J.L. Lions (Eds.), Handbook of Numerical Analysis, North-Holland, Amsterdam, 1990, pp. 197–462.
[29] G. Strang, On the construction and comparison of difference schemes, SIAM J. Numer. Anal. 5 (1968) 506–517.
[30] W.C. Chew, W.H. Weedon, A 3D perfectly matched medium from modified Maxwells equations with stretched coordinates, Microwave Opt. Technol. Lett. 7 (13) (1994) 599–604.
[31] G. Cohen, Higher-Order Numerical Methods for Transient Wave Equations, Springer, Berlin, 2002.
[32] E. Heikkola, Y.A. Kuznetsov, P. Neittaanmäki, J. Toivanen, Fictitious domain methods for the numerical solution of two-dimensional scattering problems, J. Comput. Phys. 145 (1998) 89–109.